Comparing the mechanical properties of CEM I and CEM III/B concrete in building site conditions

Experimental study and building life-cycle approach

Sander Kirillova
Studentnumber: 4654420

Graduation committee
Prof. dr. ir J.G. Rots (Chair, TU Delft)
Prof. dr. H.M. Jonkers (Supervisor, TU Delft)
Dr. ir. Y. Yang (Supervisor, TU Delft)
Ir C. Bosveld (Company supervisor, Pieters Bouwtechniek Delft)

A thesis presented for the degree of Master of Science
at the Delft University of Technology

Faculty of Civil Engineering and Geoscience
Delft University of Technology
28-06-2024

Preface

This thesis *Comparing the mechanical properties of CEM I and CEM III/B concrete in building site conditions* has been written to obtain the Masters degree in Civil Engineering at TU Delft. If you have a civil engineering background or are simply interested in the application of concrete in practice, please feel free to read this report.

During this thesis I have learned a great deal about concrete technology, the effects on different mechanical properties and how it all affects the life-cycle of a building. Besides that I am very grateful for the opportunity of conducting many experiments in the Stevinlab, where I could gain practical experience besides the theory from my master Structural Engineering.

Throughout my whole thesis I have had the support of several people. First I would like to thank my chair Prof. dr. ir. Jan Rots. From the moment I introduced this subject to you, you have always shown great enthusiasm and aided me in my decisions. Second I would like to thank my supervisor Prof. dr. Henk Jonkers. You have guided me so much with deciding on which experiments and curing conditions to use, and you were always happy to explain the practical importance of this study. Then I would like to thank Dr. ir. Yuguang Yang for being my supervisor. During the whole process you have kept on challenging me to think about the necessity of every experiment and all the research. You have also shown great interest in my experiments are provided your guidance here. For the last but not the least member from my committee, I would like to thank Ir. Chris Bosveld from Pieters Bouwtechniek. With your practical experience as an engineer I was able to make better decisions for my experiments, and you were always very interested in the results.

Besides my committee, I would like to thank Ir. Jan Versteegen and Ir. Rob Doomen from Pieters Bouwtechniek, for giving me this subject in the first place and providing me with a working space. I would also like to thank Maiko van Leeuwen and Ake Blom from the microlab and macrolab for your guidance in the experiments. It was a very nice change of pace to goof off a bit in the lab, and be reminded to not take everything too seriously. While performing the experiments I received extra guidance from Ir. Yubao Zhou and Dr. ir. Navid Vafa, whom I like to express my gratitude to as well.

Finally I would like to thank my friends and family for supporting me throughout this whole journey and providing me with the needed distractions. Especially my mother and Nienke have continuously provided me with a lot of positive energy which I am very grateful for. I am very satisfied with the end result. Please enjoy!

Sander Kirillova
Delft, July 2024

Summary

To achieve the goals set by the Paris Agreement to have a fully circular economy in 2050, sustainability will play a larger role in all aspects of life. One sector where sustainability is especially important, is the building sector. The building sector accounts for one third of the total environmental impact, so small changes go a long way [95].

In the journey of reaching the set goals, many innovative solutions are being applied. One of these solutions is the use of waste products to both limit waste, and reduce the need for raw materials. A solution in concrete that has been used frequently in maritime infrastructure, is the use of blast furnace slag cement (CEM III). This slag is a waste product of the steel industry, and can be used as a replacement for clinker. Since clinker has a massive carbon footprint, theoretically this is a solid solution. The research testing this concrete in lab conditions has been positive as well. However, the building site has a drastically different environment than the perfect conditions found in a lab. One example where the properties of the CEM III concrete have not been as expected, is the high speed line for trains in the Netherlands [100]. Due to a higher porosity, cracks and moss growth became a large problem, reducing the durability and impacting the allowed speeds of the trains. This example begs the question if applying CEM III/B, which is a standard cement type used in the Netherlands, really is as sustainable as believed. To better understand the effects of applying CEM III/B concrete instead of Portland Cement (CEM I), the following research questions have been answered:

- *What are the differences in mechanical properties for a CEM I 42.5N and CEM III/B 42.5N concrete mixture, when cured in a relative humidity of 55%?*
- *What is the total effect on the life-cycle of a building when applying these different concrete mixtures, also considering sustainability?*

A relative humidity of 55% is chosen for two reasons. First, this humidity is plausible on the building site of The Netherlands. In the winter months the average relative humidity is around 90% and in the summer 60% [99]. High wind speeds massively affect the relative humidity though. Typical Dutch winds are able to decrease the relative humidity of concrete below 60% throughout the whole year, due to the moisture loss it causes [97]. The second reason for choosing the 55% curing chamber is the limited amount of curing chambers available in the Stevinlab of the TU Delft. The weather conditions in the Netherlands suggest that a 55% relative humidity is a regular occurrence on the building site.

First research question
The main focus of this thesis has been answering the first research question, which was eventually done by experiments. The first step has been the literature study into the hydration of cement. The literature suggests that clinker has a much faster hydration than blast furnace slag, meaning that CEM I will have a higher early-age strength. Since

blast furnace slag requires clinker to hydrate first, the strength gain will be much slower. In an optimal relative humidity of close to a 100%, this is no issue. However, due to the relative humidity being only 55%, the unreacted water in the concrete is prone to evaporation. The expectations were that the evaporation will impact CEM III concrete more than CEM I concrete, due to the late hydration. The results of the experiments confirm that the mechanical properties of CEM III concrete are indeed affected more.

Based on the research questions and literature study, it was evident that a research-gap needed to be bridged. Most research has been comparing the mechanical properties of CEM I and CEM III in optimal curing conditions, in a relative humidity of nearly 100%. The conditions on the building site however, are often much worse. To obtain more knowledge on the mechanical properties in sub-optimal curing conditions, an experimental campaign was designed and conducted. These lab-tests consisted out of; Shrinkage tests, compression tests, static modulus tests, bending tests for both reinforced and unreinforced beams, and water absorption tests.

The **shrinkage test** resulted in 12% higher shrinkage for blast furnace slag concrete over a time span of 75 days. The autogenous shrinkage, which is caused by the internal movement of small fractions of water, was even twice as high. The water loss is also 18% higher, thus the higher shrinkage makes sense.

This additional water loss also resulted in a 14% additional porosity, with a total of 9.64% compared to a porosity of 8.46% for CEM I concrete.

The **cube compression tests** showed the speed of the compressive strength gain. The cubes were supposed to reach a minimum value of 42.5MPa after 28 days. The CEM I cubes easily surpassed this with an average strength of 50.27MPa. The CEM III cubes however only reached 36.45MPa. It was very noticeable that after 7 days, the cubes barely gained any strength due to not enough water being available for hydration. Some additional cubes that were cured in a 97% relative humidity were tested, and here both concrete mixes achieved a similar strength just below 55MPa. A large variance was observed in the cubes cured in 55% humidity compared to the specimen cured in 97% relative humidity.

A **static modulus test** was performed to observe the Young's modulus in compression, which resulted in 33GPa and 28GPa for the CEM III and CEM I mixture consecutively. This 18% difference can be explained by the difference in material volume. Due to the higher porosity in the blast furnace slag concrete, less hydrated concrete is available. With less material to give resistance to deformation, the Young's modulus is lower. The CEM III mixture experienced a higher variance in the results as well. It became clear that there was localised brittle failure on two sides of the specimen, while the CEM I mixture experienced a more gradual softening after the peak. This observation means that the curing conditions impact the CEM III much more.

An **unreinforced three-point bending test** with a notch, resulted in tensile Young's moduli of 38GPa and 31GPa. Both these values are higher than the E-moduli in compression, which can for one be explained by the much higher loading rate during

the test. This influences the static mechanical properties. Another explanations might be the crude approximation of the forget-me-nots used to determine the Young's moduli. The peak tensile stresses in the CEM I and CEM III concrete were 3.40MPa and 2.81MPa, meaning a difference of 21%. Due to the lower strength and more brittle behaviour, the fracture energy was 30% lower as well. These results can again be explained by the higher porosity.

A **reinforced four-point bending test** was supposed to give an indication on the bond strength between the steel reinforcements and concrete. The results were a slightly larger crack spacing for CEM I with 170mm, compared to 151mm for CEM III concrete. This was not consistent with the theory and the rest of the results, since a higher porosity should have given a worse bond. However, the placement of the reinforcements play a huge role in the results. Due to the inexperience of the author who handmade the reinforcement cages, these cages were inconsistent, thus triggering some preferential crack spacing. The quality of the steel was also irregular, meaning that there is insufficient reliability to draw generic conclusions.

Lastly, a **water absorption test** resulted in consecutively 8.46% and 9.64% porosity for CEM I and CEM III. When considering the hydration speed and water loss of CEM III concrete, it is to be expected that the porosity is higher.

The conclusion of these results, is that the mechanical properties for the CEM III concrete cured in 55% relative humidity, are about 15-30% worse when compared to CEM I in the same conditions. This is all due to the curing conditions having a bigger effect on blast furnace slag. Due to delayed hydration, there is more unreacted water available in the first days and even weeks after casting. When exposed to a lower humidity, the water evaporates, thus increasing the porosity. The porosity affects all other mechanical properties, since there are less solid particles within the concrete to provide resistance and strength.

Second research question

The life-cycle of a building consists of the production of the materials, the construction, service-life, and end-of-life phase. By comparing the production of both CEM I and CEM III, it follows that the estimated carbon footprint of CEM I is 2.5 times larger than CEM III. This is mainly due to the high temperatures involved in producing clinker.

The construction of a building using CEM III would take four times as long however to meet the necessary safety requirements. To build on a cast in-situ floor for example, 70% of the characteristic strength of the floor should be reached. Usually one week is used, which is more than sufficient for the Portland cement. The blast furnace slag concrete would need 28 days to achieve this value however. On top of that more cracks are expected, since the tensile strength and fracture energy is significantly lower.

The largest impact can be found in the service-life. Due to all mechanical properties being weaker in CEM III concrete, the risk of failure and need for maintenance increase. The durability on the other hand decreases, meaning that the intended lifespan of the building may not be reached. The higher porosity allow for easier chloride ingress that

affects the reinforcements. The lower Young's moduli allow for higher deformations, meaning higher strength concrete or larger dimensions should be used. The increased shrinkage can add stresses to the elements when movements are constrained, resulting in more cracks. Finally, the higher variance in the experimental results means that it is less predictable and thus less reliable to use.

Lastly, for the end of life of both concretes, recycling was considered. Recycling a CEM I mixture would result in a slightly higher gain, since reclaiming clinker has more worth than blast furnace slag.

To conclude the findings of this research, it can be stated that sub-optimal curing conditions affect CEM III significantly more than CEM I. Not only are the mechanical properties lower, but there is a higher uncertainty in the CEM III mechanical properties as well. Applying CEM III in sub-optimal conditions would require extra careful considerations in the treatment. In the given building site conditions, applying CEM I would be significantly more durable, cheaper, and especially safer.

Nomenclature

A	Al_2O_3 - Aluminum oxide - Alumina
BFS	Blast Furnace Slag
$C-S-H$	$C_3S_2H_3$ - Calcium silica hydrate
C	CaO - Calcium oxide - Lime
$C\bar{S}H_2$	$3CaSO_4 \cdot 2H_2$ - Calcium sulfate (Gypsum)
C_2S	$2CaO \cdot SiO2$ - Dicalcium silicate (Belite)
C_3A	$3CaO \cdot Al_2O_3$ - Tricalcium Aluminate (Aluminate)
C_3S	$3CaO \cdot SiO2$ - Tricalcium silicate (Alite)
$C_4A\bar{S}H_{12}$	$3Ca_4Al_2OH_{12} \cdot SO_4 \cdot 6H_2O$ - Monosulfate
C_4AF	$4CaO \cdot Al_2O_3 \cdot Fe_2O_3$ - Tetracalcium ferroaluminate (Ferrite)
$C_6A\bar{S}_3H_{32}$	$3CaSO_4 \cdot Al_2O_3 \cdot 3CaSO_4 \cdot 32H_2O$ - AFt (Ettringite)
CH	$CaO \cdot H_2O$ - Calcium hydroxide - Portlandite
F	Fe_2O_3 - Iron(III) oxide - Iron oxide
$GGBFS$	Ground Granulated Blast Furnace Slag
H	H_2O - Water
S	SiO_2 - Silicon dioxide - Silica

List of Figures

List of Tables

Table of contents

1 Introduction

The ever-growing population and its demand, result in more and more infrastructure being necessary. However, with the goal to achieve a fully circular economy in the Netherlands by 2050 and the building industry amounting to 1/3rd of the environmental impact, this becomes a real challenge [95]. To minimize the environmental damage done to this planet, sustainable solutions are implemented in the building of this infrastructure. But not all of these solutions are implemented with a full understanding of the material behaviour. This gap in knowledge becomes a big problem, especially when some of these sustainable solutions are already being used in practice.

Concrete is one of the most popular construction materials due to its price and workability, but the process of making clinker for cement comes with a large environmental cost. To combat this problem, several alternative materials are being used to replace part of the cement, like blast furnace slag in CEM III concrete. Blast furnace slag is a waste product from the steel industry, so implementing this will both decrease waste and the need for clinker. This results in more sustainable concretes, but also changes the mechanical properties of the concrete. Comprehensive research has already been conducted comparing CEM I and CEM III concretes in perfect lab conditions, but these conditions do not accurately represent the reality at the building sites [96]. With both humidity and wind speeds affecting the curing process, the 'sustainable' CEM III might not be so sustainable after all [97]. To make a comparison of how these two types of concrete would behave in infrastructure with cast in-situ concrete elements, they need to be compared in sub-optimal curing conditions with a lower relative humidity.

Research objective
This report will aim to gain a better understanding of both CEM I and CEM III/B concrete which is cast in-situ. CEM I has been used in buildings for a while, so extensive date is available on its behaviour. CEM III has mainly been used in maritime infrastructure, so its application in buildings is relatively new. To make reliable designs using CEM III in the future, this gap in research needs to be filled. The following research questions will aid in achieving this objective:

- *What are the differences in mechanical properties for a CEM I 42.5N and CEM III/B 42.5N concrete mixture, when cured in a relative humidity of 55%?*
- *What is the total effect on the life-cycle of a building when applying these different concrete mixtures, also considering sustainability?*

The main question that this thesis will discuss is the first one. The 55% relative humidity is chosen to simulate the building conditions in The Netherlands. The Netherlands has an average relative humidity of 90% in the winter and 60% in the summer [99]. The high wind speeds lower this humidity even more. With average wind speeds surpassing 4m/s, the internal relative humidity of concrete can even fall under 40% [104] [97]. To simulate

realistic conditions and due to the availability of curing chambers, a relative humidity of 55% is chosen. The second question will give insight on possible consequences when applying both mixtures in practice. From the production phase till the end of service life.

Report outline
These research questions will be answered using both literature research and experiments. The structure is as follows:

- Chapter 2: The chemical compositions of the two different cement mixes is explained.
- Chapter 3: The process of hydration is discussed. This process will determine all mechanical properties of the concretes.
- Chapter 4: To determine which experiments are necessary, the important mechanical properties are supported with literature.
- Chapter 5: The exact mix design for the experiments is determined.
- Chapter 6: The method for how the experiments will be conducted is demonstrated. Based on the literature research of chapter 2 till 5, the expected results are explained as well.
- Chapter 7: The results from the experiments are visualised.
- Chapter 8: The possible effects on the life-cycle of a building are given.
- Chapter 9: The results from both the experimental results of chapter 7, and life-cycle effects of chapter 8 are discussed.
- Chapter 10: A conclusion to this research is given, and the research questions are answered.
- Chapter 11: Recommendations are given for future research, and advise is given to the building industry.

Part I:
Literature Study

2 The different compositions of cement

This chapter will present the two different cement mixes studied in this Thesis. First the specifications for the CEM I and CEM III cement mix will be given. The constituents of the cements will then be discussed, ending with the chemical composition

2.1 Cement components

This section will present the two cement mixes for the experiments. The constituents of these mixes will be presented as well. The definitions of the mixes are given by the Eurocode: En 197-1.

There are two cement mixes that will be used in the experiments. The first one is CEM I 42.5N, which is a standard Portland Cement mix that is regularly used worldwide. It contains between 95-100% clinker, with 0-5% of additional constituents. The 42.5 means it has a middle strength class out of the three main strength classes of cement. The N stands for a normal strength development [14].

The second one is CEM III/B 42.5N which is Portland Cement combined with a high concentration of blast furnace slag, often used in the Netherlands. It contains 20-34% clinker, 66-80% blast furnace slag and 0-5% of additional constituents [14]. It also has a middle strength class with normal strength development. Table 2.1 gives a clear overview of the components.

Cement type	Clinker content [%]	Blast Furnace Slag content [%]	Additional constituents content [%]
Portland Cement (CEM I)	95-100	-	0-5
Blast Furnace Cement (CEM III)	20-34	66-80	0-5

Table 2.1: Composition of the cement mixes [14]

2.1.1 Clinker

Clinker is obtained by firstly combining calcareous and argillaceous materials together [20]. The calcareous material used in cement production is usually limestone, and it is characterized by its contents of calcium and magnesium [26]. The argillaceous materials are mainly silica, alumina and oxides of iron, which are found in clay or shale [20]. These raw components are then combined as a homogeneous mixture. The kiln heats the raw materials up to the sintering temperature, which means that one solid mass is created without reaching the point of liquefaction. Lastly, the solid mass is grinded into clinker in combination with gypsum [25]. Figure 2.1 gives a schematic representation of this process.

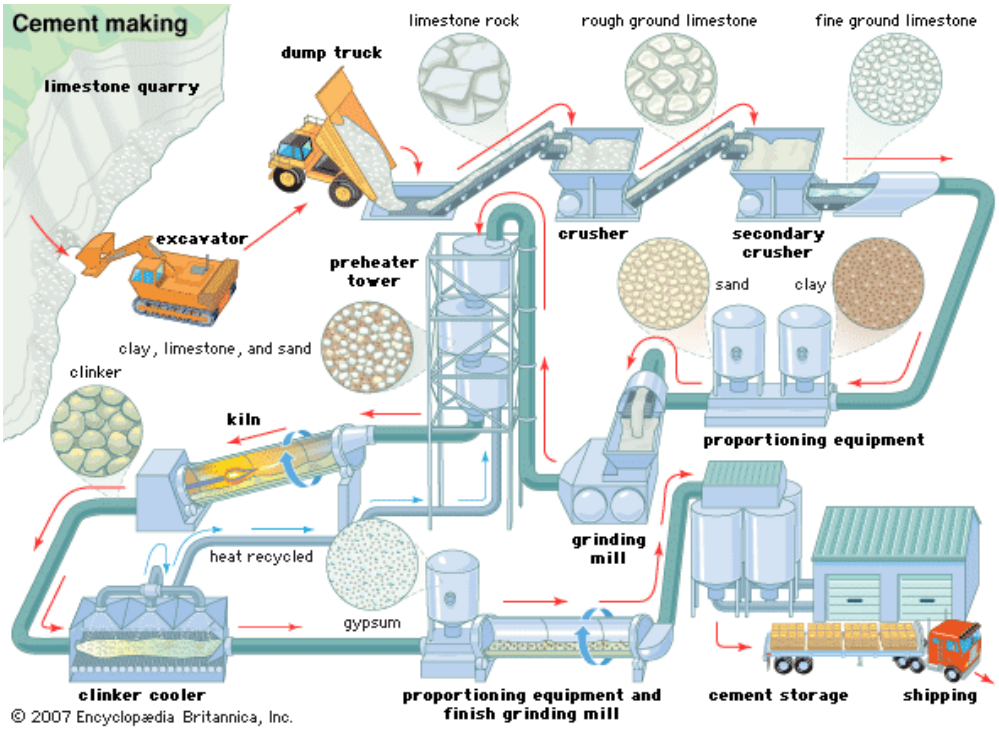

Figure 2.1: Clinker production [27]

During the process of heating up the raw materials, some chemical reactions begin to form. When the clinker reaches a temperature of approximately 900°C, the limestone and clay start reacting with each other. The last chemical reactions form at a temperature of 1400-1600°C, which gives the following constituents within the clinker [20]:

- C_3A: Tricalcium aluminates (Aluminate)
- C_3S: Tricalcium silicate (Alite)
- C_2S: Dicalcium silicate (Belite)
- C_4AF: Tetracalcium ferroaluminate (Ferrite)

The effect of each of these constituents will be explained in chapter 3.

2.1.2 Blast Furnace Slag

Blast Furnace Slag is a by-product from the manufacturing of steel and iron. It comes in multiple forms and sizes, and has different properties depending on how it is treated. The most important slag for the production of CEM III is Ground Granulated Blast Furnace Slag (GGBFS). The first step for obtaining this slag, is obtaining regular Blast Furnace Slag. A combination of iron ore and limestone is heated up in a furnace

by special metallurgical coal [29]. when a temperature of 1400-1500°C is reached, two products are created: molten iron and molten slag. Figure 2.2 gives a representation of this process.

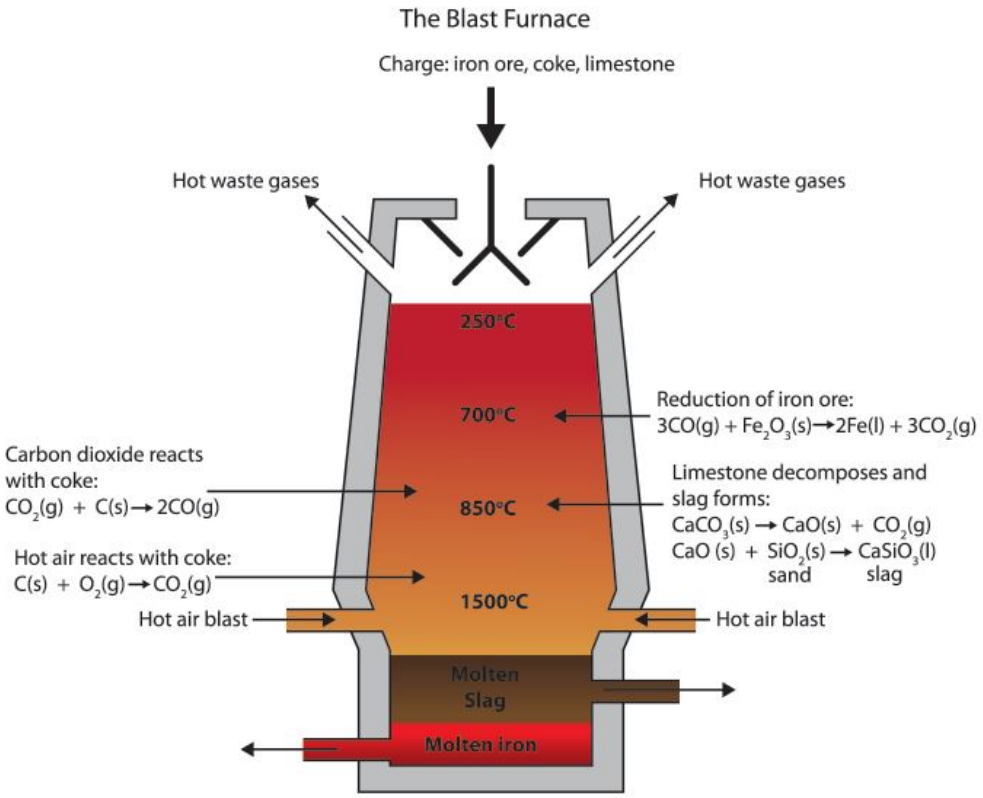

Figure 2.2: Blast Furnace Slag production [28]

As can be seen in figure 2.2, the slag lays on top of the iron due to the difference in density, and is extracted. By rapidly cooling this slag in a large volume of water, the cementitious properties are optimized [29]. By drying and grounding the slag to a fine powder, the final product of Ground Granulated Blast Furnace Slag is obtained. The effects of this slag in CEM III will be explained in chapter 4.

2.2 Chemical composition

Due to the different ways of acquiring clinker and BFS, the minerals within the CEM I and CEM III mixes differ as well. The exact chemical composition of the two types of cements can be seen in table 2.2.

Cement type	CaO	SiO_2	Al_2O_3	Fe_2O_3	MgO	Na_2O	K_2O	TiO_2	MnO	P_2O_5	SO_3	Other
CEM I 42.5N	63.12	20.32	4.60	3.24	1.92	0.26	0.61	0.44	0.07	0.35	3.20	0.12
CEM III/B 42.5N	46.21	30.67	9.09	1.17	5.55	0.20	0.70	0.80	0.13	0.05	4.93	0.52

Table 2.2: Chemical composition of CEM I 42.5N and CEM III/B 42.5N in weight percentage [15]

How these substances influence the cement and eventual concrete, will be explained in chapter 3. Mainly large differences in the calcium oxide and silica oxide can be observed.

3 Hydration of cement

The reaction between the water and cement particles is a chemical process, also called hydration. This process is of utmost importance for concrete, since it will define all mechanical properties of concrete. This chapter will first explain the importance of this reaction, followed by how it works in both clinker and blast furnace slag.

3.1 Why is hydration important

The heat rate evolution of the hydration process is significant to note for several reasons. How fast and how high the temperature of the concrete increases, greatly affects the strength and durability of the concrete. A high temperature indicates a high early-age strength, but can also negatively influence the final strength [6]. Another importance of the temperature development becomes evident when fresh concrete is poured over older concrete elements. While the young concrete hydrates, the temperature rises and the concrete expands. The old concrete restraints the young concrete from deforming, causing compression in the young concrete and tension in the old concrete. When the young concrete cools down again, the tension can be found in the young concrete and compression in the old. This can be seen in figure 3.1. This process causes unwanted cracks.

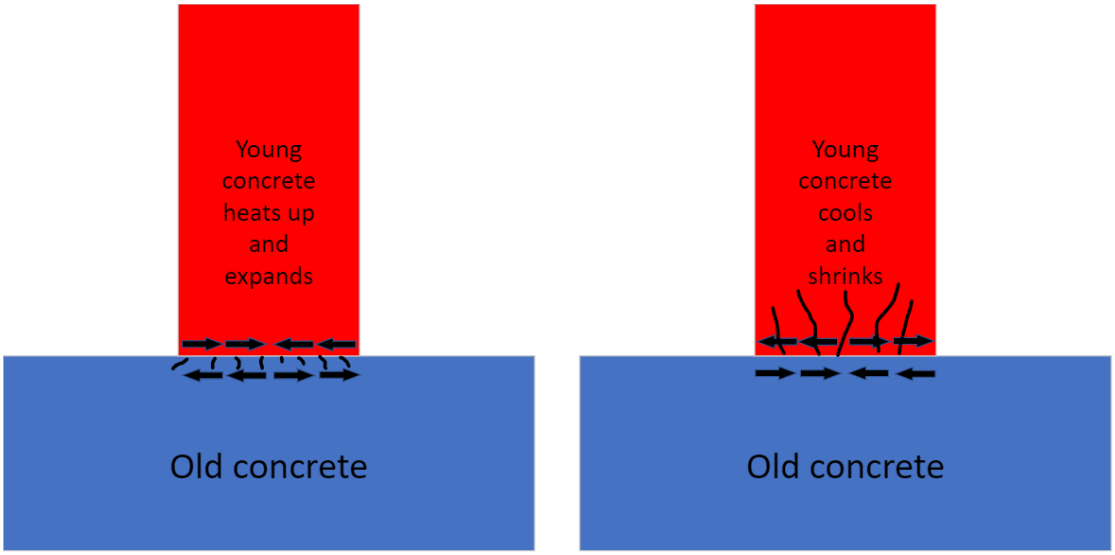

Figure 3.1: Young concrete expands and shrinks causing cracks

3.2 Hydration process

The hydration process is determined by several factors, which will be discussed in chapter 3.5. One of the most notable parameters is the composition of the cement. The

mineralogical composition of cement determines the heat rate evolution during hydration, which gives the strength and durability properties over time [15]. The mineralogical composition of both CEM I 42.5N and CEM III/B 42.5N are given in table 3.1.

	CEM I 42.5N [%]	CEM III/B 42.5N [%]
C_3S	61.2	15.4
C_2S	13.0	2.2
C_4AF	10.3	2.4
C_3A	4.4	1.4
Anhydrite	4.7	2.5
Calcite	2.7	0.6
Dolomite	1.2	2.2
Bassanite	0.8	0.7
Quartz	0.5	0.2
Periclase	0.5	-
Aphthialite	0.4	-
Portlandite	0.2	-
Gypsum	0.1	1.2
Amorphous	-	71.3

Table 3.1: Mineralogical composition in weight percentage [15]

The most notable minerals of the cements are C_3S, C_2S, C_4AF, C_3A, gypsum and the Amorphous, since they contribute to the hydration [20]. The Amorphous mineral comes from the blast furnace slag. These components react with water, starting a chemical reaction where heat is released. When C_3S and C_2S react with water, they start forming a strong 'glue' to bind the aggregates together. This glue is called Calcium Silica Hydrate (C-S-H) and accounts for the majority of the concrete strength [33]. This can be seen in equations 3.1 and 3.2.

$$2C_3S + 6H \rightarrow C - S - H + 3CH \tag{3.1}$$

$$C_2S + 4H \rightarrow C - S - H + CH \tag{3.2}$$

The difference between the two, is that C_3S hardens rapidly and accounts for the early strength. C_2S hardens slowly, and gives strength to the concrete beyond one week [35].

C_3A and C_4AF do not form C-S-H, but still partially contribute to the overall strength. They both hydrate very quickly, which means that they mainly contribute to the early age strength. This quick reaction is unwanted however, since the concrete will set too soon [35]. Additionally, the reaction between C_3A releases a lot of heat. To retard this process, gypsum is added in the cement mix. When combined with enough gypsum in the early stages of hydration, ettringite ($C_6A\bar{S}_3H_{32}$) is formed. Ettringite is a mineral that is purely useful for controlling the setting time, since it forms a protective layer around the cement particles to hinder the C_3A hydration [34] [37]. The following formulas show

the reactions of the before-stated components with water. If gypsum is present:

$$C_3A + 3C\bar{S}H_2 + 26H \rightarrow C_6A\bar{S}_3H_{32} \tag{3.3}$$
$$C_4AF + 3C\bar{S}H_2 + 30H \rightarrow C_6A\bar{S}_3H_{32} + FH_3 + CH \tag{3.4}$$

If all the gypsum is used up but ettringite is available:

$$2C_3A + C_6A\bar{S}_3H_{32} + 4H \rightarrow 3C_4A\bar{S}H_{12} \tag{3.5}$$
$$2C_4AF + C_6A\bar{S}_3H_{32} + 12H \rightarrow 3C_4A\bar{S}H_{12} + 2CH + 2FH_3 \tag{3.6}$$

If all gyspum and ettringite is used up:

$$C_3A + 6H \rightarrow C_3AH_6 \tag{3.7}$$
$$C_4AF + 10H \rightarrow C_3AH_6 + CH + FH_3 \tag{3.8}$$

The final important reactions come from the BFS. BFS is both hydraulic and pozzolanic. The latter means BFS reacts with CH in the presence of water [36]. The reaction is as follows:

$$Amorphous + CH + H \rightarrow C - S - H \tag{3.9}$$

All the above-mentioned reactions occur at different times during hydration and release heat. Based on the amount of heat that is released, the hydration process can be divided up into five stages. These different stages of heat evolution can be found in figure 3.2.

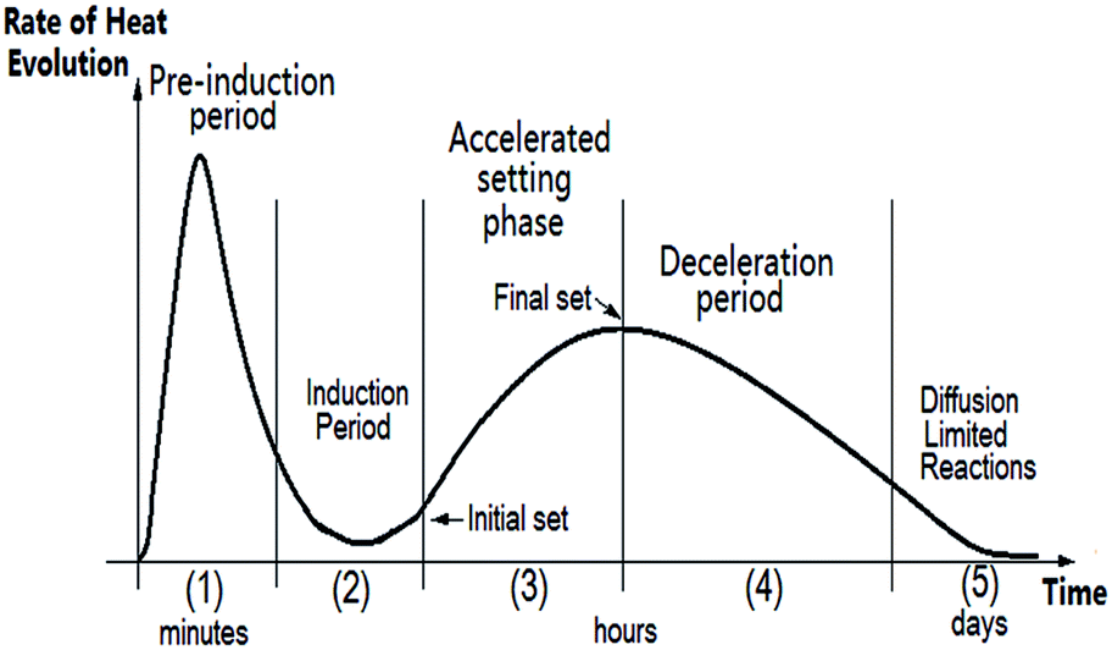

Figure 3.2: Heat evolution of fresh concrete [32]

In the **Pre-induction period** the highest rate of heat evolution can be seen in figure 3.2 within minutes. This can be explained by the quick reaction of C_3A and C_3S both giving off large amounts of heat during hydration [39]. Since the reaction product of C_3A is unwanted, gypsum is used to retard this process. At the end of the Pre-induction period, the heat rate goes down significantly. There are many theories that try to explain the reason, however only the 'Dissolution' theory is able to explain every single detail [39] [40] [41] [42]. When calcium particles within the cement start to react with water, the amount of Ca^{2+} ions in the water solution is increased. At some point the solution becomes supersaturated, meaning that the ions are not able to dissolve anymore. This leads to a solid reaction product being formed surrounding the cement particles, and thus temporarily preventing further hydration [39].

The surrounding of the cement particles leads to the **Induction period**. Almost no reactions are occurring in this stage, which means it is the perfect time to transport the concrete to the building site. To both maintain the homogeneity and delay further hydration, the truck has a mixer drum which can rotate [43].

The **Accelerated setting phase** starts once the protective layers are being destroyed. Like the name states, this stage signifies the beginning of the setting of concrete. All reactions from equations 3.1 and 3.2 continue. Depending on the amount of gypsum and ettringite available, hydration of C_3A and C_4AF continue based on equation 3.3, 3.4, 3.5, 3.6, 3.7 and 3.8.

In CEM III, most of the BFS is activated after the clinker of the Portland Cement has started reacting [38]. This can also be seen when inspecting equation 3.9. Some of the BFS contains C_3S as well, but most of the slag needs lime (C) to start forming C-S-H. This lime is produced in the form of Portlandite (CH) when the clinker starts reacting, like can be seen in equation 3.1 and 3.2. The result is that the slag has quite a late reaction compared to the other minerals, thus it contributes most to the late-stage strength. The peak of the Accelerated setting phase is skewed more to the right as well for CEM III/B compared to CEM I, due to this late reaction [20].

In the **Deceleration period** large amounts of hydration products are formed. These products start to form barriers around unhydrated cement particles, making it harder for those to come into contact with water. This means that the rate of reactions start slowing down, as can be seen in figure 3.2.

The last stage is called **Diffusion limited reactions**. The reactions slow down tremendously, and are mainly controlled by diffusion. Since particles move at random, some particles that are within a C-H-S layer can reach the outside. Due to the randomness, this process takes days, months or even years. An example of diffusion of C_3S can be seen in figure 3.3 [45]. The reaction keeps going till either all the cement particles or water have been used, or the internal Relative Humidity lowers to about 80% [20]. The importance of Relative Humidity will be further explained in chapter 3.5.

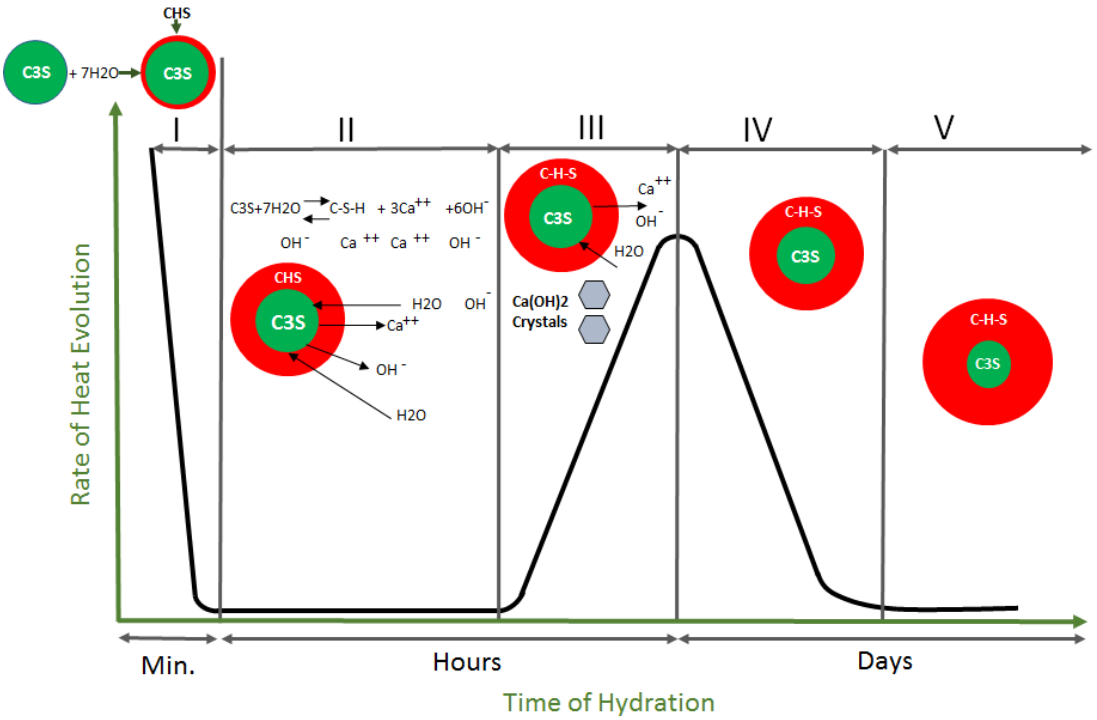

Figure 3.3: Diffusion of C_3S [45]

3.3 Voids during hydration

Besides the solid hydration products in the cement paste, there are also voids influencing its properties. During hydration the solids are constantly moving around, causing multiple kinds of voids [24]. The moving of these solids can cause shrinkage and creep, so it is important to get an understanding of this principle. The different pore-sizes are given in figure 3.4, and all bring different consequences.

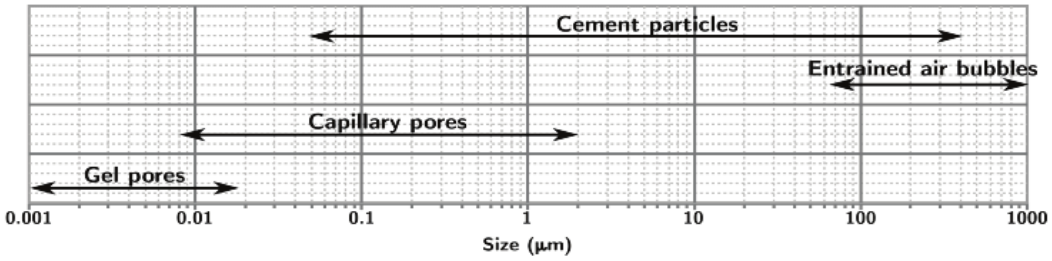

Figure 3.4: Ranges of void sizes within cement paste [24]

The **Gel pores** refer to the pores between the C-S-H sheets, and range from 1-20 nm. There are two major studies describing these pores, which are performed by Powers and

Brownyard [47] and Feldman and Sereda [48]. Both suggest that the void sizes are too small to affect the strength and permeability. The water within the gel pores might have an affect on shrinkage however, which will be further elaborated in chapter 3.4.

Capillary pores are significantly larger than Gel pores, and represent the voids between hydrated solid cement [49]. A clear visual is given in figure 3.5.

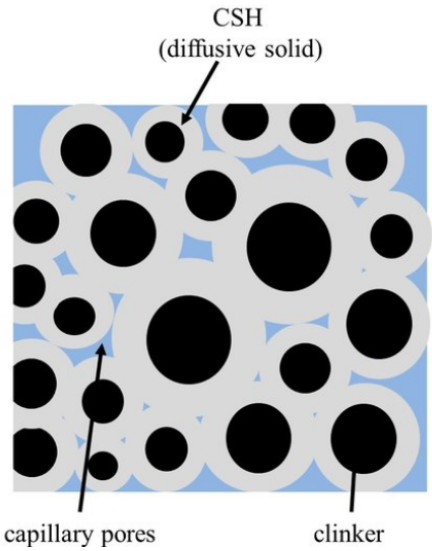

Figure 3.5: Capillary pores [49]

The distribution of these pores is determined by the water-to-cement ratio, and the degree of hydration (i.e. the fraction of cement that has fully reacted with water relative to the total amount of cement in the sample) [24]. It is important to note that the volume within the cement paste does not really change during hydration, if the relative humidity is high enough. During casting, the water will flow through the cement particles causing them to separate from each other. When the w/c ratio is high, the spaces between the cement particles become larger as well. This can be seen in figure 3.6.

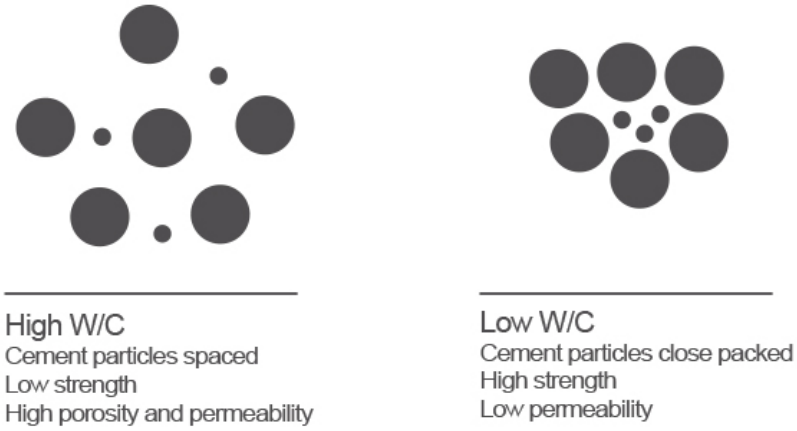

Figure 3.6: Effect of w/c ratio [50]

To understand why this influences the capillary pores so much, it is important to note two things:

- For every $1cm^3$ of cement, $2cm^3$ of hydration product can be produced.
- The distances between the cement particles do not really change much during hydration

This means that if the space between the cement particles is too large, the voids can not be filled by the hydration products, since the amount of hydration product every cement particle can form is limited. The result is that high w/c ratios cause more capillary pores than lower w/c ratios [47]. Assuming that the hydration reaches a 100%, the result will be as stated in figure 3.7. Seeing how much volume capillary voids might fill, this amount can heavily influence both the strength and permeability of the concrete, as well as the shrinkage.

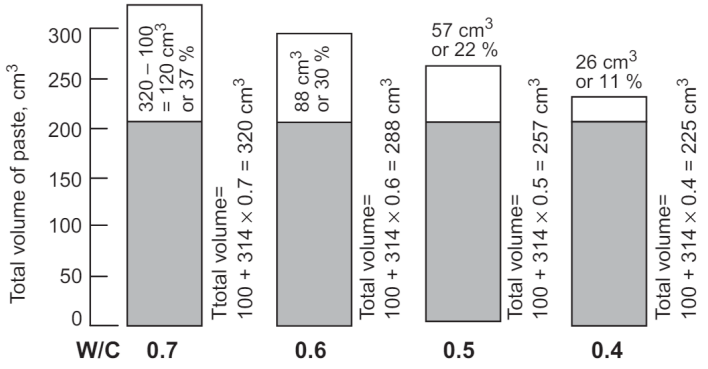

Figure 3.7: Effect of different w/c ratios on capillary pores assuming $100cm^3$ of cement [24]

The largest pores are **Air bubbles**, and can reach a size in the order of magnitude of millimeters [24]. They are typically spherically shaped, hence the name air 'bubbles'. Some air bubbles are purposely added into the mixture to protect the concrete against freeze-thaw cycles [9]. These types of voids are called 'entrained air', and are usually obtained by using some kind of admixture. Some voids are caused by improper mixing and compacting, which gives 'entrapped air'. These types of air bubble are usually larger, but can be avoided by proper vibration of the concrete. Both entrained and entrapped air can adversely affect the strength.

3.4 Water behaviour during hydration

Like already stated in section 3.3, not all water is used up when hydrating the cement. There are many forms where water can exist in the hydrated cement paste, as can be seen in figure 3.8:

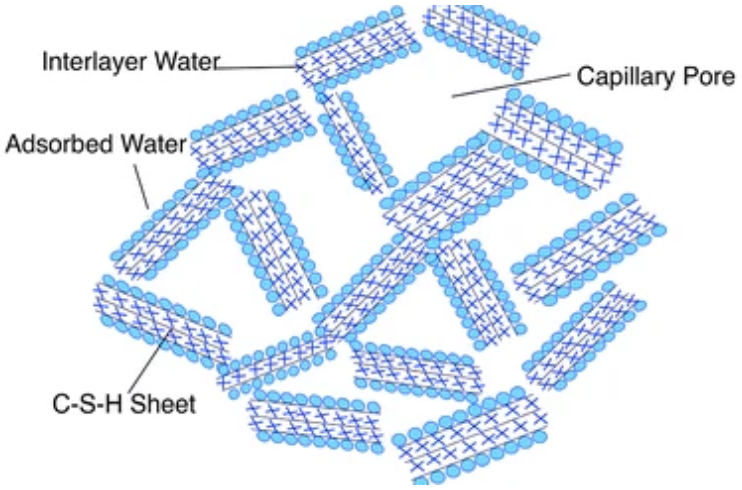

Figure 3.8: Forms of water in hydrated cement [51]

Between the layers of the C-S-H structure, **Interlayer water** can be found. This water is held strongly in place by hydrogen bonding between the C-S-H layer and the water. Since this bond is so strong, It is only lost in the case of strong drying in a relative humidity of 11% or less [24].

Capillary water can be found in the large voids, like capillary pores and air bubbles. Capillary water can be divided into two categories:

- Water in large voids ($> 50nm$): This water is free from the influence of attractive forces, and can thus be seen as 'free' water. When this is removed from the concrete, no volume change is caused.

- Water in small voids $(5 - 50nm)$: Water is attracted to the sides of the solid particles due to surface tension [52]. This means that smaller voids cause capillary tension. The removal of this water may cause shrinkage. The relevance of shrinkage will be discussed further in chapter 4.1.2.

Adsorbed water is water laying on the surface of a solid. Due to the hydrogen bonding between the water, up to six molecular layers of water can be held [24]. The further the distance between the water molecules and the solid surface layer, the lower this bond is. When the relative humidity is lowered to 30% this bond can be lost, causing shrinkage.

3.5 Parameters affecting hydration

The hydration process mainly depends on the following major factors; The relative humidity, temperature, the cement composition, w/c ratio and of course time [21]. Accelerators can also be added to a cement mix, which will influence the setting time. This is not taken into account for this Thesis however.

Relative Humidity (RH) can have quite significant effects on the hydration, since it affects the water within concrete [31]. A low RH leads to high evaporation, which leads to less available water for hydration. Moist curing gives the perfect conditions, since the RH is close to 100%. The effects of curing in a lower humidity can be seen in figure 3.9.

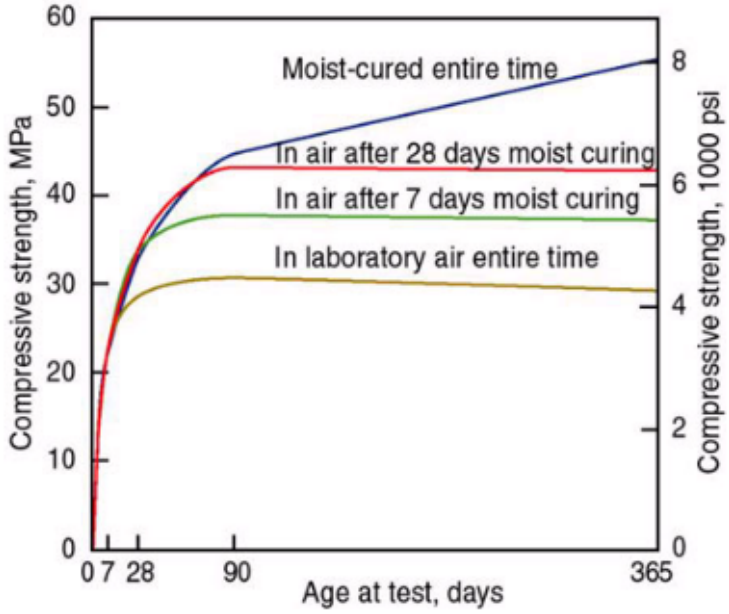

Figure 3.9: Effects of curing on compressive strength [18]

The relative humidity is influenced by both temperature and wind speed. Since the

Netherlands often experiences a lot of wind, it is interesting to see its effects in figure 3.10.

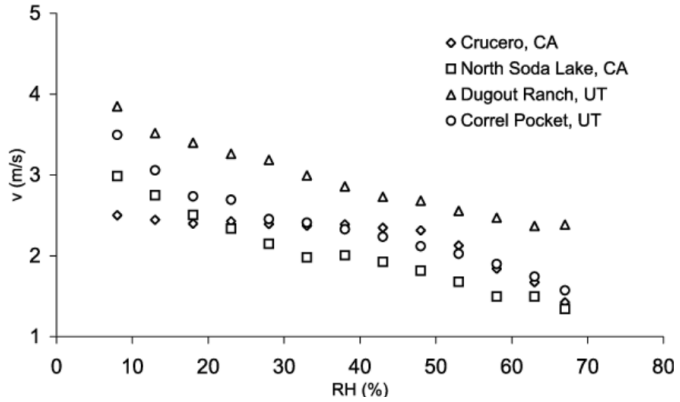

Figure 3.10: Effects of wind speed on relative humidity [97]

Temperature often plays an important role in the strength development of materials. When freshly cast concrete is put in a warm environment, the hydration process will be quicker. When the temperature is too cold however, hydration might not occur at all [19].

Cement composition has a substantial effect on hydration. These effects are discussed in detail in chapter 3.2.

w/c ratio majorly affects the amount of available water for the cement to react with. If too little water is used, the cement will not hydrate fully, thus not reaching its full capacity. If the w/c ratio is too high, the concrete will become more porous. Further information on the effects of the w/c ratio are given in chapter 3.3.

Time might play one of the most important roles in concrete hydration. Simply put, hydration requires time. Some minerals react quite fast to give an early-age strength to the concrete, but other minerals have much slower reactions. To properly utilize all the available minerals, enough time should be given for the hydration.

4 Mechanical properties of concrete

The sustainability of a material is heavily dependent on its properties. To get an understanding of which experiments need to be conducted, the most important concrete mechanical properties will be discussed in this chapter. Some other important properties of concrete will not be discussed, like fire resistance, creep, aggregates and more. These fall outside the scope of this Thesis.

4.1 Shrinkage

Determining how much a concrete element will shrink is quite important for the integrity of the element and its surroundings. Early stage shrinkage can cause cracks on the surface of the concrete. In a later stage when more of the structure is finished, shrinkage can cause major issues. Especially if a concrete element has restricted movement, the imposed deformation of the shrinkage can cause additional loading to the structure. This may lead to irreversible damage being done to the structure and in the worst case even, total collapse. Three types of shrinkage will be considered; Plastic, drying, and autogenous. The effect of these three types of shrinkage will be discussed in the section. Other common types of shrinkage like carbonation will not be considered, due to the relatively low impact [20].

4.1.1 Plastic shrinkage

Plastic shrinkage happens in the first one to eight hours after casting concrete, when the state of the concrete is still 'plastic' and not fully hardened [12]. It is the escape of surface water that is necessary for the strength gain of concrete. The water either evaporates into the atmosphere or is absorbed by the aggregates [4] too fast, so that rising bleeding water can not replace the moisture loss. Bleeding is a common phenomenon in fresh concrete, where the heavier aggregates settle down and water rises to the surface. In low rates, this usually does not pose any problems to the strength of the concrete [11]. Since the surface water can not be replaced fast enough, the surface concrete shrinks more than the interior containing plenty of water. This can be seen in figure 4.1. This causes a similar effect as can be seen in figure 3.1, where tensile stresses occur in the surface layer. Besides giving the concrete some unaesthetic surface cracks, this type of shrinkage does not really influence the strength of the concrete [13]. It does however allow for moisture and other aggressive substances to penetrate the concrete easier.

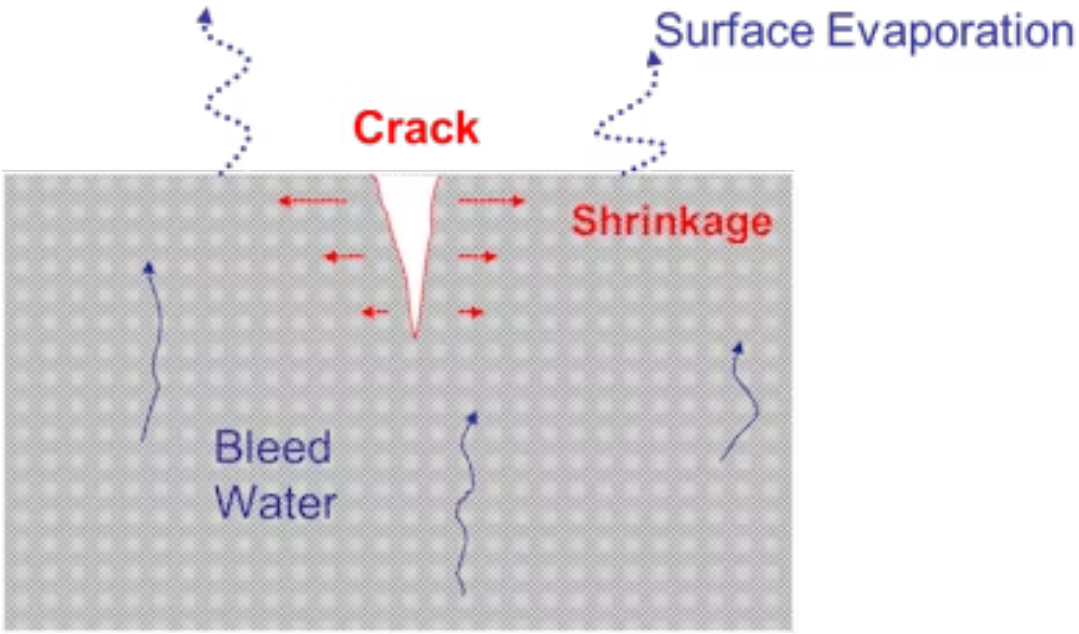

Figure 4.1: Plastic shrinkage causing surface cracks [30]

Since plastic shrinkage is mainly caused by fast evaporation of surface water, it is more likely to occur on warm, dry and windy days. It can quite easily be prevented though by covering the surface of the fresh concrete, curing the concrete with plenty of water and proper vibration during mixing [12].

On the building site, plastic shrinkage can thus become an issue when the curing process does not take into account the weather conditions. Since this Thesis mainly addresses the mechanical properties and not chemical attacks on the concrete, the plastic shrinkage effects are not taken into account. To avoid this type of shrinkage, all concrete specimen in the experiments will be covered with a plastic sheet for one day.

4.1.2 Drying shrinkage

Drying shrinkage occurs after the setting time has been reached, which means the concrete has left the plastic stage and has become solid. The largest portion of drying shrinkage occurs within the first three months of casting, while some concrete mixes need even less time [23]. As the name suggest, drying shrinkage is caused by drying of the water within the concrete. Due to the relative humidity in the atmosphere being lower than the relative humidity within the concrete, free water starts to evaporate.

Not all water loss impacts drying shrinkage however. This phenomenon happens mainly when adsorbed water and capillary water from smaller capillary pores are lost [76].

Water in larger capillary pores is relatively free to move, hence the reason it is called 'free water', like stated in chapter 3.4. When confined to narrow spaces, adsorbed water causes a repulsive force. The removal of this force removes the disjoining pressure, leading to shrinkage [20]. This concept is illustrated in figure 4.2.

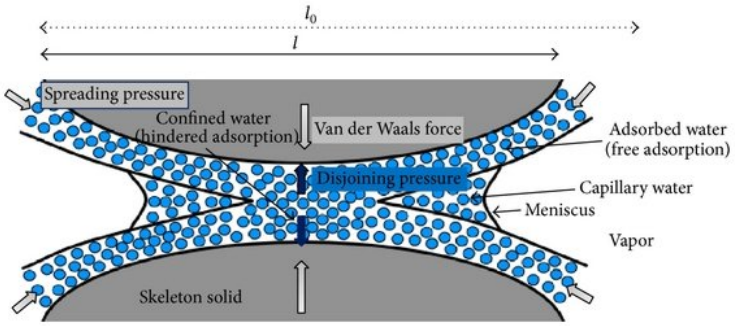

Figure 4.2: Disjoining pressure of adsorbed water [77]

Water in smaller capillary pores (5 to 50nm) is attracted to the sides, which is called capillary tension [20]. Removal of this water causes compression stresses and thus shrinkage. On top of loss of capillary water, a loss of interlayer water between C-S-H layers causes shrinkage as well. This would require a relative humidity of below 15% however, which is quite unlikely to occur [20].

To make it more complicated, the drying of concrete does not have to be uniform throughout its cross-section. This is mainly important for larger elements. Due to non-uniform moisture in concrete, shrinkage gets a differential in the cross-section of the concrete element. This differential type of shrinkage may cause tensile stresses, which in turn leads to cracks [22].

4.1.3 Autogenous shrinkage

Autogenous shrinkage is pretty comparable to drying shrinkage in many ways. This type of shrinkage is also caused by the movement of adsorbed water and capillary water. However, unlike drying shrinkage, the water is not evaporated but stays within the concrete. The movement of the water is caused by the hydration of cement. When unhydrated cement pulls in water, the previous bond of the water is lost. Like already stated for drying shrinkage, this loss of bond causes pressure and thus shrinkage [20].

When looking at the pore structure of BFS concrete, it is evident that it will be affected much more by autogenous shrinkage compared to CEM I concrete. Due to the large amount of small capillary pores, a loss of water will cause a loss of bond more often,

leading to shrinkage [53].

Even though autogenous shrinkage might cause issues, theoretically it should not pose problems for well-cured concrete. Autogenous shrinkage for a w/c ratio larger than 0.45 is often smaller than 100 microstrain, so not very noticeable [54]. For lower w/c ratio however, the majority of the total shrinkage comes from autogenous shrinkage. In improper curing conditions the same effects might be found.

Besides shrinking, concrete can **Swell** as well. This usually happens in the first 24-48 hours after mixing. The swelling often produces a negligible strain compared to the shrinkage, and occurs due to the temperature rising during hydration [55].

4.2 Young's modulus

The Young's modulus, otherwise known as the elastic modulus or E-modulus, is the property that measures the stiffness of a material. It is extremely important for controlling the displacement of structures. Since the Young's modulus is a mechanical property, it supposedly has the same value for both compression and tension [69], at least for the elastic part. Experimental results show a slight difference however, with the compressive E-modulus being slightly higher [73]. The behaviour in tension and compression differ a lot as well. This can be seen when looking at the stress-strain curve given in figure 4.3. The elastic modulus can be determined by the slope of the stress-strain curve. Figure 4.3 illustrates how the E-modulus is the same for both compression and tension in the elastic stage, even though concrete is much weaker in tension.

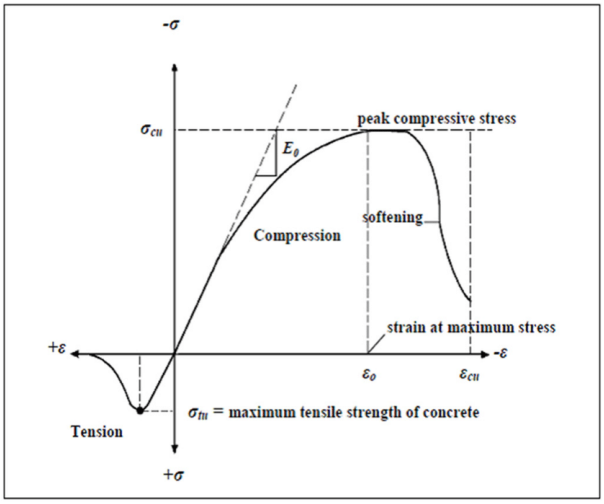

Figure 4.3: Stress-strain curve in tension and compression [70]

The Young's modulus depends on the micro-structure of the material, which means that the curing conditions play a considerate role [72]. The more compact a material is, the

steeper the slope in the stress-strain curve, thus the higher the Young's modulus. Fully hydrated BFS cement produces denser concrete, which means that typically CEM III concrete has a slightly higher E-mod [74].

4.3 Poisson's ratio

The Poisson's ratio is the relation between the transverse and longitudinal strain [75]. A good example where the Poisson's ratio is evident, is when pulling on an elastic band. In the direction of pulling, so the longitudinal direction, the band is elongated. The width in the transverse direction is then shortened however. This phenomenon is especially important for the crack behaviour. When concrete is compressed in the longitudinal direction, tensile stresses are formed in the transverse direction. The cracks from the tensile strain depend on the Poisson's ratio. Just like the Young's modulus, its value depends on the micro-structure of the material [72]. The expression for the Poisson's ratio can be defined as the transverse strain divided by the longitudinal strain. This can be seen in equation 4.1.

$$\nu = \frac{\epsilon_t}{\epsilon_l} \tag{4.1}$$

4.4 Compressive behaviour

One of the most notable characteristics of concrete is its compressive strength. There are many factors which play a role in the compressive strength over time like the cement mix, aggregate distribution, w/c ratio, temperature and humidity. Like described in chapter 3, these factors all influence the hydration process and consequently the strength properties.

Softening
Besides the compressive strength, softening behaviour in pure compression is important to determine as well. Softening can be described as the decrease of strength with an increasing deformation [62]. This happens when the concrete leaves the elastic stage, and starts deforming permanently, like can be seen in figure 4.4. This deformation can be caused by a multitude of fracture modes, like splitting, spalling or shear fracture [105]. The higher the slope of the softening, the more brittle the material is. A more ductile behaviour of concrete can be desirable for the structural safety.

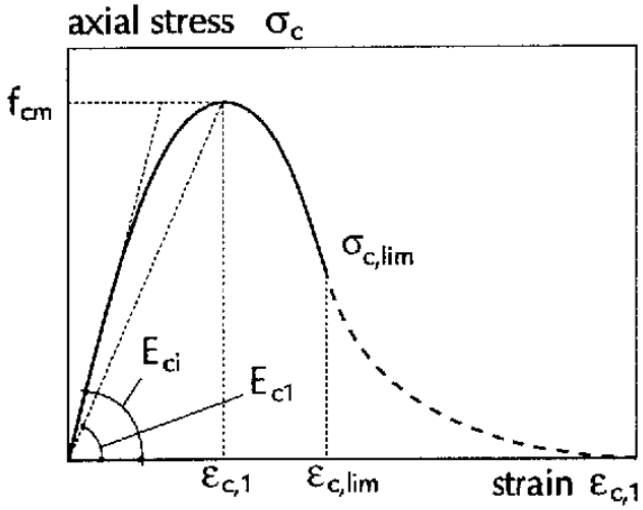

Figure 4.4: Softening behaviour of quasi-brittle materials like concrete [63]

Softening can be explained by the cracking behaviour of concrete. **Uni-axial** compression causes tensile strains in transversal directions and vice versa, like demonstrated in figure 4.5. These tensile strains cause cracks. At first the cracks are at micro-level, which means that the integrity of the concrete is still intact. At peak load unstable macro-cracks start forming. These macro-cracks cause discontinuities at structural level, resulting in the concrete having a heterogeneous response instead of homogeneous. This causes the stresses in the concrete to be nonuniform, resulting in progressive failure of the internal bonds, otherwise known as softening.

Since the macro-cracks are unstable, the load has to be decreased. To really see the softening behaviour, the concrete should thus be tested in a displacement-controlled setup and not load-controlled.

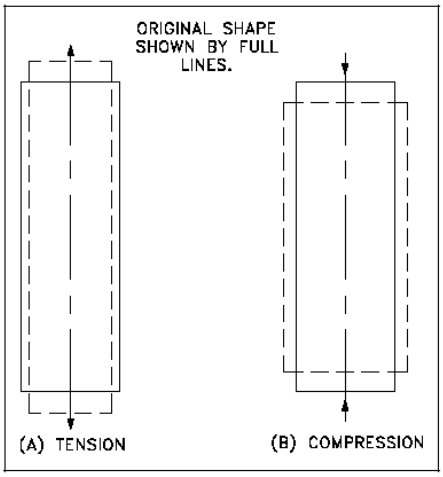

Figure 4.5: Longitudinal strains causing transversal strains [65]

4.5 Tensile behaviour

Just like the compressive strength, the tensile strength is influenced by the hydration process. In practical calculations, the tensile strength of concrete is often neglected due to its relatively small and unreliable contribution to the overall strength of a structure. Even though the tensile strength is not considered in the calculations, it is often the case that a concrete element is under tension in some part of the cross-section at some point in time. The reinforcements make sure that the elements will not fail, but still the concrete will show cracks. The tensile properties become important for the damage propagation. If the concrete easily forms large cracks, it can lead to water and chlorides being able to reach the reinforcements. This can lead to corrosion, which is a major problem for the integrity of a concrete element. Since the plastic strains are caused by tensile forces, softening becomes important here as well. The relevance can be found in chapter 4.4.

Fracture energy
Besides the tensile strength, the fracture energy is quite important to understand the cracking behaviour of concrete. Fracture energy is expressed as the energy required, to open a unit area of the crack [83]. In other words, it can be expressed as the energy a material can absorb while cracking. This energy depends on the work being done to cause fracture, which is equal to the displacement in one direction, times the force in the same direction. If a force - displacement graph is plotted, the work is equal to the area underneath the graph. This is demonstrated in figure 4.6. This work divided by the crack area results in the fracture energy. The crack area is equal to the width of the beam, multiplied by the height of the crack.

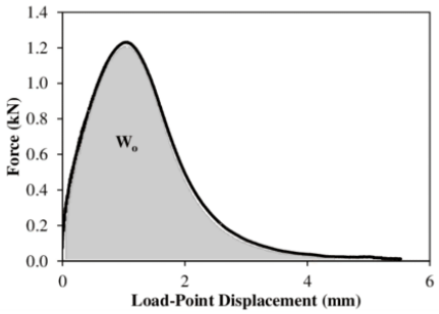

Figure 4.6: Fracture energy [84]

It can be seen that the fracture energy thus relies on the maximum force, which in turn leads to the tensile stresses, and the softening behaviour of the material.

The fracture energy is a size-dependent parameter. In the standard RILEM testing procedure, it becomes evident that the notch height, the ratio of the notch height and

beam height, and aggregate size all affect the fracture energy majorly [86].

4.6 Porosity and Permeability

The porosity and permeability of concrete greatly affect its strength and durability. Even though these two terms are not the same, they are interconnected.

Porosity
The degree of porosity depends on the volume of capillary pores. Like said in chapter 3.3, these pores are highly dependent on the hydration process [33]. Pores signify the absence of solid material, which means that the strength is influenced. Besides decreasing the strength, a high porosity can give other problems like freeze-thaw. When the water retained in the pores freezes, it expands thus causing internal stresses. These stresses can lead to micro-cracking [67].

The porosity can be calculated by dividing the volume of the water in the pores by the total volume of the specimen [68], like described in equation 4.2:

$$\phi = \frac{V_w}{V_t} * 100 \tag{4.2}$$

Permeability
When a concrete is permeable, gasses and liquids like water are allowed to flow through relatively easily. When these gasses and liquids are able to reach the steel within the concrete, its strength and durability can be affected heavily. Chlorides and water are examples of substances that affect the steel. The concrete itself can be influenced by intrusion as well. Some examples of this are silica reactions and carbonation.

The permeability depends heavily on the porosity, and can be described by the pore morphology [46]. When the capillary pores are large, water penetrates easier. If the pores are also interconnected, then the water can reach great depths of the concrete. Figure 4.7 demonstrates this.

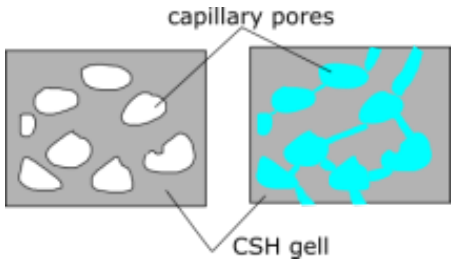

Figure 4.7: Permeability signified by the connectivity of pores [66]

The permeability can be determined by finding the permeability coefficient (k) of a

material. Darcy's law describes the behaviour of a steady state flow into a fluid, and can be rewritten into the following expression of equation 4.3 [68]:

$$k = Q\frac{L\mu}{A\Delta p} \tag{4.3}$$

Q signifies the rate of fluid flow, L is the height of the specimen, μ is the dynamic viscosity of the fluid, A is the cross-sectional area and Δp is the pressure gradient.

Relation
Like stated before, porosity and permeability and interrelated, but not linearly. The relation between the porosity and permeability factor have been determined in multiple experiments, with the results given in figure 4.8.

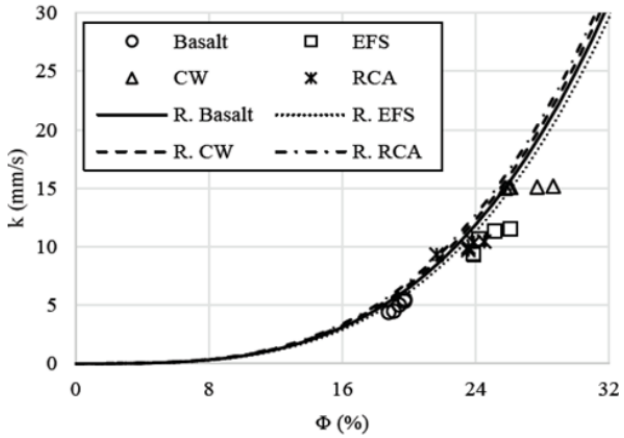

Figure 4.8: Relation between porosity and permeability [68]

5 Concrete mix design in practice

This chapter will discuss the concrete mix design in practice. First the importance of the consistency will be explained, so that the mix design of this Thesis can be calculated. When the mix design is known, the Eurocode will be used to determine its strength. At the end the curing conditions in practice will be discussed, again accentuating the difference between theory and practice.

5.1 Consistency

The consistency of freshly poured concrete has two main effects [57]:

- It can determine the strength, durability and overall performance of concrete, which means that it will actually impact all properties of the plastic concrete. All these other properties will be discussed in the rest of chapter 4.
- The workability is directly affected, which is necessary to ensure proper filling near restricted areas, and provides a better homogeneity in the concrete [5].

There are four major contributors to the workability; W/C-ratio, aggregate type, admixtures/additives and temperature [58]. A higher W/C-ratio will increase the workability significantly. Plasticizers like fly-ash will have a similar effect, but will not decrease the compressive strength as much [64]. A warmer/colder climate will increase/decrease workability as well. The aggregates can have an impact in multiple ways. First the size is important, since larger aggregates decrease the total surface area, which increases workability. On top of that, different types of aggregates can absorb more or less water, which will influence the W/C-ratio [58].

5.2 Concrete mix design

Besides the cement mixture, the water-to-cement ratio and the aggregate distributions are important factors for the strength of the concrete. The goal of these experiments is to mimic the building site conditions, which means the before-mentioned parameters will be based on these conditions. Typical w/c ratios range from 0.4-0.6, so an average value of 0.5 will be used [8]. The aggregate sizes that will be used are 0-4mm sand and 4-16mm gravel. These are also typical sizes, and are readily available near the experimental setup used. The exact distribution within the sand and gravel are not known exactly, since there is a constant supply of new aggregates which changes the distribution. The distribution will thus also be different every time new concrete is cast. Due to the availability of the aggregates, the final concrete mixture will consist out of 40% sand and 60% gravel. This is also consistent with building practice, where for every two parts of sand, three parts of gravel are used [16]. When looking at the Dutch specifications of the Eurocode, this division in sand and gravel is consistent with area I of figure 5.1.

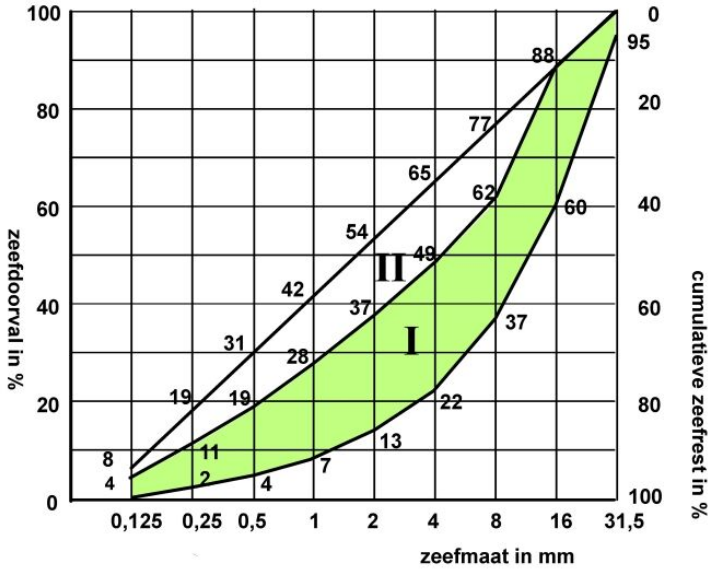

Figure 5.1: Sieving distribution [10]

Using this sieving distribution and the maximum aggregate size of 16mm, the amount of water per cubic meter of concrete can be determined. At the building site, a plastic and wet consistency is preferable. This results in 190kg of water being necessary per $1m^3$ of concrete according to figure 5.2. Plasticizers may also be used to increase the workability instead of water, but this will not be taken into account during this Thesis.

Grootste zeefmaat (mm) →	8		11,2		16		22		32	
Ontwerpgebied → / Consistentie ↓	I	I+II	I	I+II	I	I+II	I	I+II	I	I+II
droog (verdichtingsmaat ≥ 1,46)	155	175	150	170	145	165	140	160	135	155
aardvochtig (zetmaat ≤ 40 mm, verdichtingsmaat ≥ 1,26)	170	190	165	185	160	180	155	175	150	170
half-plastisch (zetmaat 50 t/m 90 mm)	185	205	180	200	175	195	170	190	165	185
plastisch (zetmaat 100 t/m 150 mm)	200	220	195	215	190	210	185	205	180	200
Voor hogere consistenties zijn geen richtwaarden gegeven. Een hogere consistentie mag alleen met behulp van een (super)plastificeerder worden verkregen, dus niet door meer water toe te voegen.										

Figure 5.2: Water mass per m^3 of concrete [10]

Besides the materials used in the mixture, concrete always contains voids as well. The mix will be based on the assumption that the air content is 3%. Typical air contents range from 3-7%, which is necessary for the concrete to be freeze-thaw resistant [9]. However a higher air content results in lower strength as well. In practice a value of 2-3% is usual, so 3% is used for the calculations. The air content varies based on the used aggregates, w/c ratio, mixing time, mixing speed and more. Since all these parameters can not a 100 per cent be recreated for each experiment, an assumption is necessary. During the experiments the actual air contents will be checked. The materials used and their density's are given in table 5.1.

Material	Density $[kg/m^3]$
Water	1000
Air	1.29
Cement	3000
Sand	2600
Gravel	2600

Table 5.1: Density concrete materials

Based on the given information thus far, the exact measurements of the mixture can now be designed:

$$V_{water} = \frac{m_{water}}{\rho_{water}} = \frac{190}{1000} = 0.190m^3$$

$$m_{cement} = \frac{m_{water}}{w/c} = \frac{190}{0.5} = 380kg$$

$$V_{cement} = \frac{m_{cement}}{\rho_{cement}} = \frac{380}{3000} = 0.127m^3$$

$$V_{aggregates} = 1 - V_{water} - V_{cement} - V_{air} = 1 - 0.19 - 0.127 - 0.03 = 0.653m^3$$

$$V_{sand} = V_{aggregates} * 0.4 = 0.257m^3 \rightarrow m_{sand} = \rho_{sand} * V_{sand} = 2650 * 0.257 = 671kg$$

$$V_{gravel} = V_{aggregates} * 0.6 = 0.386m^3 \rightarrow m_{gravel} = \rho_{gravel} * V_{gravel} = 2650 * 0.386 = 1007kg$$

For these calculations above, quite some assumptions have been made. It is for example unknown how much water will be absorbed by the aggregates, or how much water they already contain. etc..

Material	Volume [m^3]	Mass [kg]
CEMI 42.5N and CEMIII/B 42.5N	0.127	380
Water	0.190	190
Air	0.030	0
Sand	0.257	671
Gravel	0.386	1007
Total	1	2248

Table 5.2: Specifications design mix per m^3 of concrete

5.3 Strength design

According to the Eurocode, the practical strength of this mix design should reach a value between 42.5MPa and 62.5MPa [59]. However, material strength always contains some uncertainty. It can be said that 99% of the time, the compressive strength will surpass 42.5MPa. A probability density curve can be plotted for the strength, using a normal distribution with an average of 52.5MPa. This can be seen in figure 5.3.

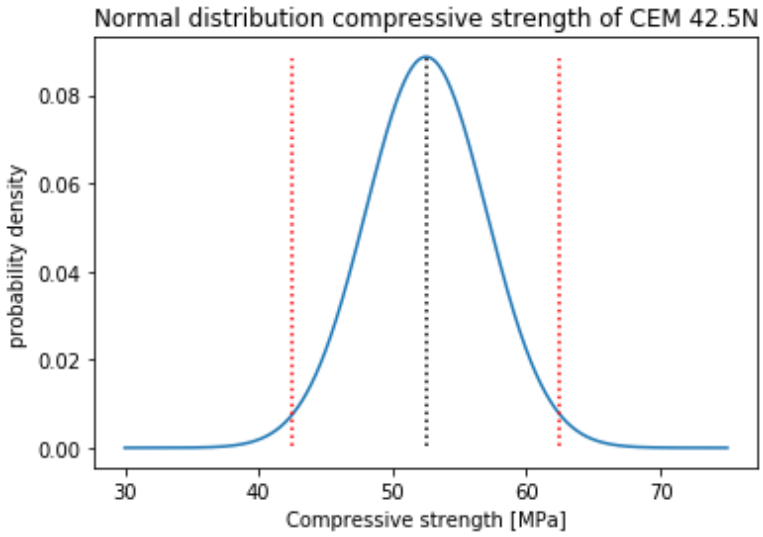

Figure 5.3: Distribution of compressive strength of CEM 42.5N concrete

5.4 Curing conditions in practice

The curing conditions majorly impact the integrity and strength that concrete will reach. More explanations of how curing may affect the material properties are given in chapter 3.

Many experiments comparing CEM I and CEM III have been using 'perfect' curing conditions, where the concrete can reach its optimal properties. This is however not in line with the building conditions on the construction site. That may result in unreliable

infrastructure when not taking the sub-optimal curing conditions into account. Like can be seen in figure 3.9 in chapter 3, the differences are not to be neglected. By using the practical expertise of the engineering firm 'Pieters Bouwtechniek', some realistic curing conditions have been set, which will be used for the experiments.

A contractor starting a new civil project, naturally wants to limit the costs. One factor majorly impacting the costs, is the labour. The longer it takes to build the specific infrastructure, the more expensive it is. The natural result of that is to speed up the building process in any way possible. There are several options for speeding this process, which all have consequences:

- Freshly poured concrete is not being vibrated enough. This leads to a higher volume of air voids.
- The concrete is not being treated properly against the weather conditions for long enough. Depending on the weather conditions, this may heavily influence how much the concrete will shrink and how porous the material becomes. This will affect the mechanical properties.
- The formworks are removed too soon, thus exposing the concrete to the environment sooner. This again influences the hydration process and thus the mechanical properties

Based on the experience at Pieters, the concrete specimen for the experiments will be covered in protective sheeting, to avoid too much bleeding. After one day, the sheets will be removed like is often done in practice. Then the specimen will immediately be placed in the 55% humidity chamber, trying to mimic the conditions of the building site. The formwork is removed within two days.

Part II:
Experimental program and results

6 Experimental setup

Based on the literature study conducted, it is evident that the curing conditions will greatly affect the micro- and macro-structure of concrete. Most research comparing CEM I 42.5N and CEM III/B 42.5N in concrete mixtures have been using 'perfect' curing conditions, where the relative humidity is kept at nearly 100%. However, research comparing these concretes in sub-optimal curing conditions, which come closer to the conditions of a building site, is limited to mainly shrinkage tests. To get a better understanding of the safety and sustainability of applying these cements in practice, a more extensive research should be conducted. By comparing multiple mechanical properties of the concretes cured in building site conditions, this knowledge-gap between existing literature and *what needs to be known* can be overcome.

In this chapter the experimental setup for every conducted test will be given. The chosen experiments are based on the material and mechanical properties that are important, to determine the durability. First the testing method will be given for every test, which is followed by the expected results.

6.1 Approach

Before performing the experiments, the literature study performed in chapters 2 till 4 will be used to determine what experiments are necessary. The combination of this literature and the availability of experimental setups in the Stevinlab at the TU Delft, determine the conducted experiments. The literature study will also help predict the results from the experiments.

The main difference between concrete testing in the lab and the concrete produced on the building site, is the curing conditions. In the lab, the perfect concrete samples can be produced by controlling the temperature, relative humidity and compaction. On the building site the conditions are often quite far from perfect though, which greatly affects the quality and properties of the concrete according to the literature of chapter 4.

Goal
To understand the behaviour of both CEMI and CEMIII concrete on the building site, the concrete samples will be cured in imperfect conditions. The temperature will be kept at 20°C, and the relative humidity at 55%. These conditions will not perfectly mimic the conditions at the building site, since these are way too inconsistent. However, performing the experiments under imperfect curing conditions will give a good indication of the qualitative difference between CEM I and CEM III used in infrastructure.

6.2 Shrinkage test

These tests will determine both the drying and autogenous shrinkage of the specimen. All specimen will be cured in a relative humidity of 55% and temperature of 20°C. The

specifications are shown in table 6.1, with the used mould in figure 6.1. The testing days are based on the properties of shrinkage. In the beginning the most shrinkage will occur according to chapter 4.1, and over time this process will slow down. The measurements will thus be made every day in the first days or even weeks, and then slow down depending on the results.

Cement type	Length x Width x Height [mm]	Amount of specimens	Shrinkage type
CEM I 42.5N	80 x 80 x 280	3	Drying
CEM III/B 42.5N	80 x 80 x 280	3	Drying
CEM I 42.5N	80 x 80 x 280	3	Autogenous
CEM III/B 42.5N	80 x 80 x 280	3	Autogenous

Table 6.1: Specifications of the specimens for shrinkage test

Figure 6.1: Shrinkage specimen while curing

Method

Since two different types of shrinkage will be tested, two types of specimen will be used as well. Figure shows the four different kind of specimen that are used. The specimen that are left uncovered are used to measure the **total shrinkage**. This total shrinkage is equal to drying and autogenous shrinkage put together. The contribution of the drying shrinkage can be found by subtracting the autogenous from the total shrinkage.

The wrapped specimen are used to measure autogenous shrinkage. This type of shrinkage is caused by the hydration of cement within the specimen, which means that the process is internal. To make sure that only the autogenous shrinkage is measured, a wrap of aquaplan bitumen sealing tape covers the concrete. This will keep the water inside to avoid drying. All types of specimen can be seen in figure 6.2.

Figure 6.2: Shrinkage specimen

The actual test is performed by using the measuring stand from figure 6.3. Before any measuring day, a steel tube with length of 280mm will be used as a zero-measure. Using this constant zero-measure, the relative length of the specimen will be measured.

Figure 6.3: Shrinkage test setup

To accurately place the specimen in the testing setup, each specimen has a bolthole. The attachment from the setup will hold the specimen in place at the bolthole, so that the shrinkage will be tested at the same spot repetitively. The autogenous specimen have a small cut within the sealing tape to uncover the bolthole. Figures 6.4a, 6.4b and 6.4c give a visual representation.

(a) Drying specimen **(b)** Autogenous specimen **(c)** Attachment to bolthole

Figure 6.4: Shrinkage specimen connection to machine

Expected result
Since CEM I concrete will hydrate quicker, it is expected that less free water will be available. That will result in the drying shrinkage being smaller compared to CEM III concrete. Later on CEM III concrete will experience more drying shrinkage however, so the end results is expected to be quite similar. The autogenous shrinkage of CEM III however is expected to be much higher due to its pore structure. Like stated in chapter 4.1.3, the BFS decreases the pore size and increases the discontinuity in the pore structure while hydrating. The capillary water is then sucked into the small voids, causing local compressive stresses. This in turn leads to autogenous shrinkage. According to the literature presented in 4.1.3, the autogenous shrinkage of CEM III concrete can be twice as high as CEM I concrete, so this is also expected.

Since the specimen used for testing autogenous shrinkage have a small cut at the top and bottom, they are slightly exposed to the environment. This means that drying shrinkage might also impact these specimen ever so slightly.

6.3 Compression test

To determine the compressive strength development over time for the specific concrete mixture used in this thesis, cube compression tests are conducted. The specifications of the used specimen are described in table 6.2.

Cement type	Length x Width x Height [mm]	Amount of specimens	Relative humidity
CEM I 42.5N	150 x 150 x 150	10	97%
CEM III/B 42.5N	150 x 150 x 150	10	97%
CEM I 42.5N	150 x 150 x 150	18	55%
CEM III/B 42.5N	150 x 150 x 150	18	55%

Table 6.2: Specifications of the specimens for cube compression test

The specimens placed in the 55% relative humidity chambers are used to mimic the site conditions during a civil project. The 97% humidity results will be used as a comparison. Figure 6.5 shows the condition of the cubes within the first day of casting. After this, the cubes are demoulded and placed in their respective chambers.

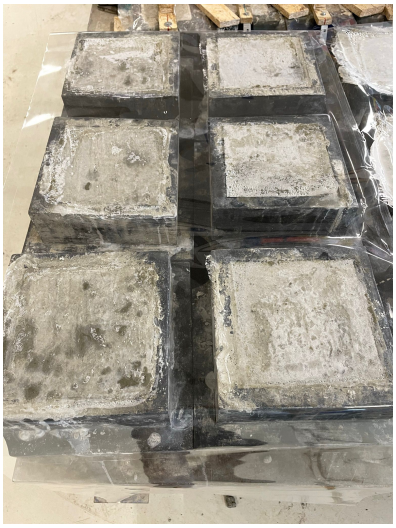

Figure 6.5: Concrete cubes for compression test

Method

The tests are performed using the compression machine of the Stevinlab at the TU Delft. In the case of the 55% relative humidity cured samples, the tests are performed at 1, 3, 7, 14, 28 and 56 days after casting. For the 97% humidity samples only the 56th day is excluded. Three specimen are used on every testing day to improve the reliability of the results for the 55% humidity. Only two cubes are tested each day for the 97% humidity concrete cubes, since this data is simply used to verify the benefits of proper curing.

The tests will be executed using the 'Automatic Compression Test' function. This means that the increase in load over time is constant and can not be manually controlled. The increase in load is recommended to be 13.5kN/s for this specific machine, so this value will be used. This also means that the test is force controlled. Once the compressive strength starts to decline consistently, failure has occurred and the test is stopped automatically. The setup can be seen in figures 6.6a and 6.6b.

(a) Starting point **(b)** Failure

Figure 6.6: Compression test setup

Expected result

According to the literature research of chapter 4, both the CEM I and CEM III mixture should reach a similar compressive strength between 42.5MPa and 62.5MPa, with a high probability of reaching between 50MPa and 55MPa according to chapter 5.3. However, this is only the case for the specimen cured in a nearly perfect relative humidity of 97%. It is also very likely that the CEM I concrete will have a significantly higher early age strength. The large amount C_3S in CEM I will hydrate rapidly, and thus reaches a higher strength faster. After several days to weeks, most of the C_3S will have hydrated, thus slowing down the hydration. The amorphous material in CEM III needs the byproduct CH from other reactions to activate, which happens after C_3S and C_2S have started hydrating.

The samples cured in 55% relative humidity will experience significantly more water loss compared to a 97% humidity. This will hinder the hydration process especially in the later stages, due to the compounding effect of the water loss. Since the CEM I samples gain most of their strength in the beginning, it is expected that the water loss will not impact its strength significantly. Perhaps the 28-day compressive strength will be at the lower end of the 50-55MPa, so around 50MPa. The CEM III samples on the other hand gain their strength much later, so these will be affected greater. The 28-day strength is expected to be around 45MPa, which is slighty higher than the minimum it

should theoretically reach. It is likely that the strength gain will massively slow down after a few weeks, since the available water keeps on reducing. The first few weeks it is expected that the 55% and 97% humidity specimen will have similar strength gain. A summary of the expected results is given in table 6.3.

Cement type	Relative humidity	Strength development	Final strength
CEM I 42.5N	97%	Massive strength gain in the first week. Will then slow down, while still gaining some strength.	Between 50-55MPa
CEM III/B 42.5N	97%	Medium strength gain in the first week. Will then slow down slightly, while gaining significant strength.	Between 50-55MPa
CEM I 42.5N	55%	Massive strength gain in the first week. Will then slow down compared to 97% humidity.	Around 50MPa
CEM III/B 42.5N	55%	Medium strength gain in the first week. Will then slow down hard compared to 97% humidity.	Around 45MPa

Table 6.3: Expectations for cube compression test

6.4 Static modulus test

The static modulus test determines both the Young's modulus and Poisson's ratio. The set-up for the Poisson's ratio is unfortunately broken however, so this will not be measured. The cuboids from the shrinkage test will be used in this setup. These cuboids have been undergoing shrinkage for 90 days at the time of testing.

Method

The shrinkage samples will have metal points attached to them, like can be seen in figure 6.7a. These points allow for the LVDT's to be attached, which will measure the displacement. The displacement is achieved by applying a compressive strain of $0.015mm/s$. Figure 6.7b shows the complete setup with the LVDT's in place. These are placed at all four sides of the concrete, to get an average displacement of the cuboid. The placement at all four sides will also provide information on how the concrete fails. The Poisson's ratio could be determined by placing a square cage around the concrete

to measure the transversal displacement during compression. This cage is not available unfortunately.

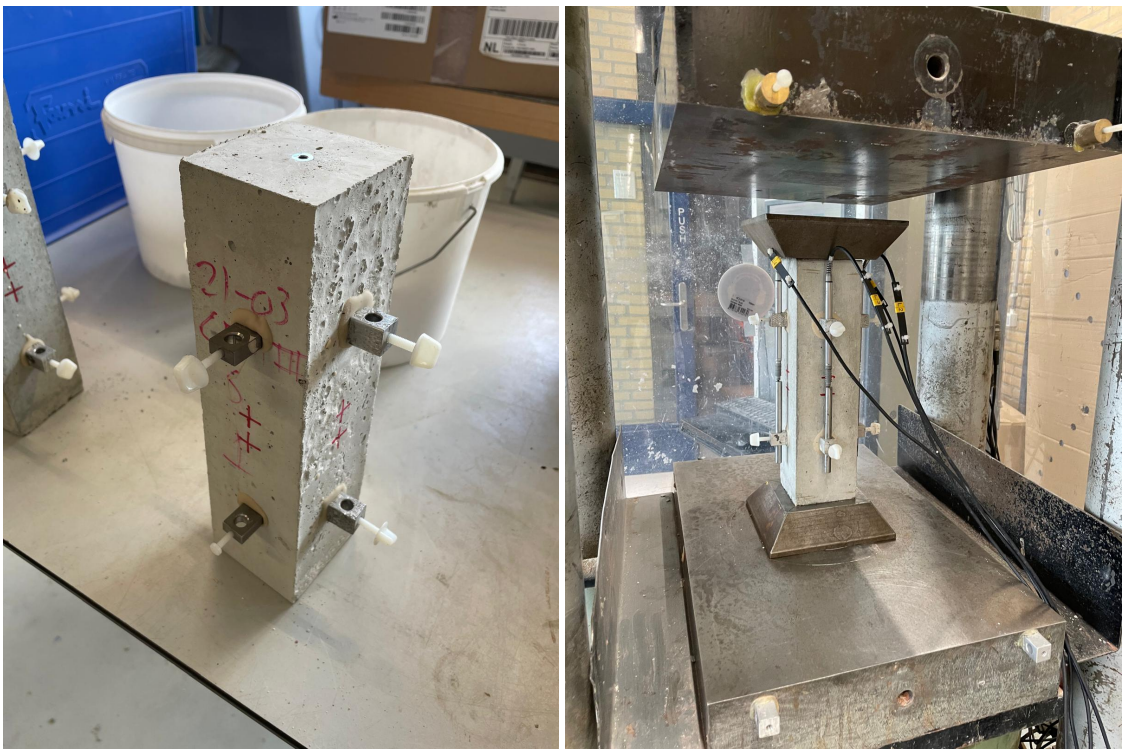

(a) Specimen **(b)** Test set-up

Figure 6.7: Static modulus test set-up

Expected result
Since the expectations for the concrete cube strength fall at approximately 50 MPa, this falls in line with the C40/50 category of the Eurocode [71]. The code assigns a value of **35 GPa** to the modulus of elasticity of a C40/50 concrete. Thus it is expected that the CEM I concrete will obtain a value around 35. The expectations for the CEM III concrete compressive strength is around 45 MPa. This gives an expected E-modulus of 33 GPa.

The standard Poisson's ratio according to the Eurocode is 0.2 [71]. This can not be tested unfortunately.

6.5 Workability test

Like stated in chapter 5.1, a workable concrete mixture is necessary to ensure homogeneity. There are multiple ways to test the workability, like a slump test or flow table test [57]. However, due to the many years of practical experience of the concrete worker of the TU Delft lab, these tests were deemed unnecessary.

Method
The expert will ensure the workability by visual inspection, based on the many years of practical experience. It is quite hard to achieve the exact same concrete mix repeatedly, due to the moisture content in the aggregates and mill being different every time. The concrete worker has many years of experience however, and can achieve quite a consistent mix.

Expected result
The concrete will be kept in the rotating mill, until all the aggregates are covered with a layer of cement paste. An example of what the mixture will look like is shown in figure 6.8.

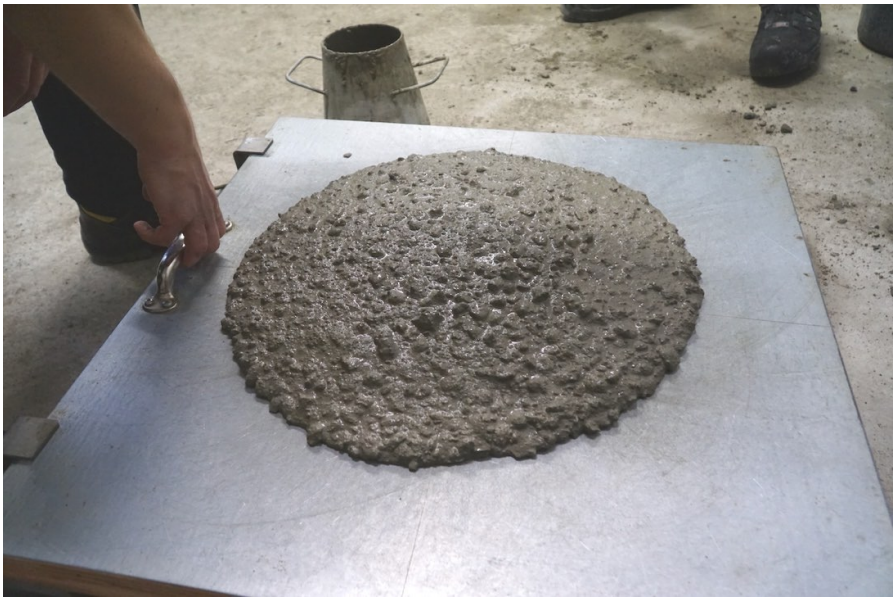

Figure 6.8: Visual inspection of workable concrete

6.6 Unreinforced three-point bending test

The three-point bending test is performed to evaluate three different properties; The tensile strength, the fracture energy and the young's modulus. The specifications of the specimen are given in table 6.4 below.

Cement type	Length x Width x Height [mm]	Amount of specimens
CEM I 42.5N	1900 x 200 x 300	1
CEM III/B 42.5N	1900 x 200 x 300	1

Table 6.4: Specifications of the specimens for three-point bending test

The specimen also have a **notch** of 30mm in height and 10mm in width. When testing the girder, the cracks will start forming from the weakest point bearing the highest

load. Implementing a notch will make sure that the weakest point is known, so that the crack propagation can be followed accurately. The height of the notch has been determined by the literature study of Murthy et al. (2013), where the effect of notch height compared to the beam depth has been analysed [78]. The conclusion of this study is that both the beam height and notch-to-depth ratio affect the fracture energy drastically. However, using a correction based on multiple other studies, these factors will not affect the fracture energy results [79] [80] [81]. Then it becomes important to use a ratio which will allow for the most accurate testing, which can be achieved with a high tensile strength. To make sure that the tensile strength of the specimen are as high as possible, the smallest notch height-to-depth ratio will be used from the literature study. The notch height-to-depth ratio is 30mm / 300mm equals 0.1. The width does not really influence the properties, but a width of 10mm is necessary for the formwork. A piece of timber with the dimensions of the notch will be attached to the formwork to obtain the dimensions given in figure 6.9. The placement of the supports and load is given as well.

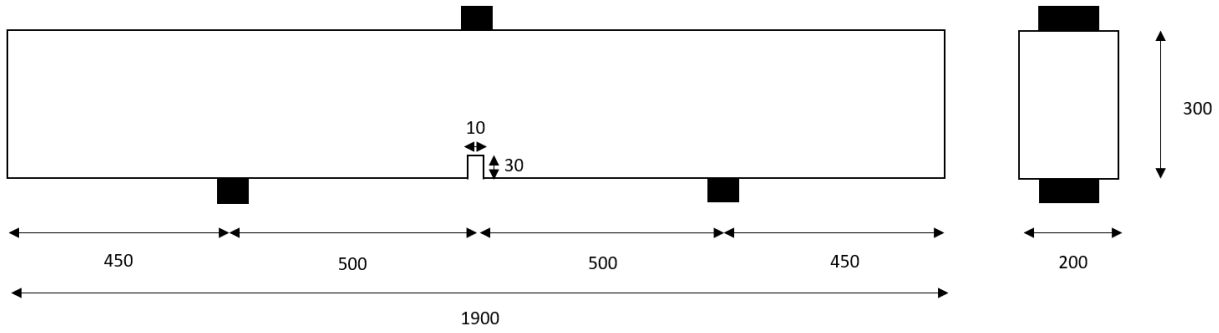

Figure 6.9: 3-point bending test setup

Method

The notched girders will be placed in the 100kN setup of the Noordhall in the Stevinlab of TU Delft. One of the supports will be a rolling support, while the other will be a regular hinge. Linear Variable Differential Transformators (LVDT's) are placed at the bottom and on the side of the specimen to measure the strains, like can be seen in figure 6.10a [61]. To get even more accurately results, Digital Image Correlation (DIC) is also installed on the other side of the girders, like can be seen in figure 6.10b. Using a flashlight which reflects on the paint, the position of the pixels can be determined with every picture. By continuously making pictures during the test, the displacement of the pixels can be determined. The vertical displacement will be measured using a laser, according to figure 6.11.

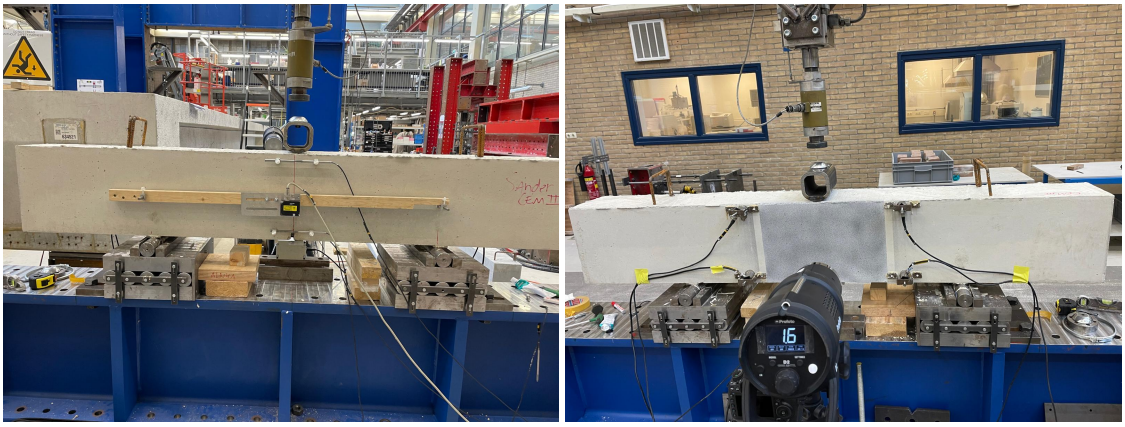

(a) LVDT side **(b)** DIC side

Figure 6.10: Three-point bending test setup

Figure 6.11: Laser

The laser is placed at the center of the beam, since there is no strain at the neutral axis of a cross-section.

The **tensile strength** will be determined by the following formulas:

$$f_t = \frac{M * z}{I} \tag{6.1}$$

$$I = \frac{1}{12} * b * h^3 \tag{6.2}$$

$$M = \frac{1}{4} * F * L \tag{6.3}$$

The moment of inertia is simply determined by using the width and height of the girder at the cross-section of the notch. The distance z will also be used for this cross-section. The length used for calculating the moment is the distance between the supports, which comes out to one meter. By continuously increasing the load until failure is reached, the tensile strength can thus be determined.

The **Young's modulus** can be found by using the forget-me-nots based on the fibre-model. This model states that the fibres in the neutral axis do not deform, and thus have no stresses. This is a crude model, but deemed accurate enough for the goal of this Thesis, which is comparing the CEM I and CEM III concretes. The formula is as follows:

$$w = \frac{F * L^3}{48 * E * I} \tag{6.4}$$

The deflection in the middle of a span depends on the parameters given above. This deflection will be measured using a laser, so that the young's modulus can be determined at all times.

The final property that this test will determine, is the **fracture energy**. This can be done in two different ways. The first option is to place either an LVDT or clip gage right underneath the notch, so the crack propagation can be measured. When the crack starts opening more and more, the LVDT or gage moves accordingly. This means that the gage will show the maximum width of the crack. Due to the availability of LVDT's, this will be used. The second option would be to not use either a laser or LVDT to measure the deflection of the center of the beam at each loading point. According to the RILEM procedure, this can also give the fracture energy, like described in chapter 4.5. It is opted to use the first method, due to the simplicity in data processing for this method. To get the optimal stress-strain curve, the test will be performed based on the crack width. A constant crack-width rate of 0.002mm/s will be used to guide the force. The LVDT measuring the crack width will send feedback to the hydraulic cylinder, so that this rate can be maintained.

Expected results
The expected result for the Young's modulus in tension is comparable to the comressive one. This was estimated to be around 33-35GPa. The expected strain in tension is around 100 microstrain [82]. Assuming the linear relation determined by Hooke's Law, the tensile stresses can be determined. Equations 6.5 and 6.6 show the tensile stresses of the CEM I and CEM III concrete mixtures.

$$f_{t_I} = 35000 * 100 * 10^{-6} = 3.5MPa \tag{6.5}$$

$$f_{t_{III}} = 33000 * 100 * 10^{-6} = 3.3MPa \tag{6.6}$$

Due to the dependence on notch height, beam height and aggregate size, it is hard to predict an exact value for the fracture energy. Most importantly, the two different

concrete mixes should be comparable. The softening curve of the CEM I concrete is expected to be more ductile compared to the CEM III concrete, due to the porosity. When taking into account the higher expected tensile stress as well, the fracture energy of CEM I should also be higher.

6.7 Reinforced four-point bending test

The four-point bending tests are mainly performed to get an idea of the crack spacing, which will reflect on the bond between the reinforcements and the concrete. The specifications of the specimen are given in table 6.5.

Cement type	Length x Width x Height [mm]	Amount of specimens
CEM I 42.5N	1900 x 200 x 300	1
CEM III/B 42.5N	1900 x 200 x 300	1

Table 6.5: Specifications of the specimens for four-point bending test

These girders will have both longitudinal and vertical reinforcements. The stirrups are mainly centered between the support and load, to prevent shear failure. Three additional stirrups are placed within the two loading plates to provide overall stiffness to the reinforcement cage. The longitudinal reinforcement on the bottom is the minimum required reinforcement according to the Eurocode. This comes to 3 bars placed 65mm apart. Two longitudinal bars are placed on the top as well, to provide stiffness to the reinforcements. All bars have a diameter of 10mm.

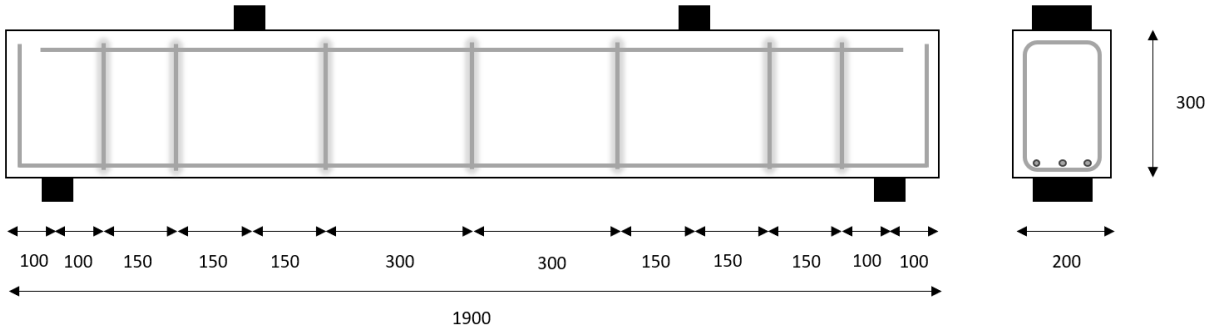

Figure 6.12: 4-point bending test setup

Method

The setup for the four-point bending test is nearly identical to the three-point bending test. Figure 6.13a and 6.13b show the LVDT and DIC side. A laser is used to measure the deflection as well.

(a) LVDT side **(b)** DIC side

Figure 6.13: Four-point bending test setup

Expected results

The crack spacing can be calculated using the Eurocode formula given in equation 6.7 [56].

$$S_{r_{max}} = k_3 * c + k_1 * k_2 * k_4 * \frac{\phi}{\rho_{s_{eff}}} \tag{6.7}$$

k_1 takes into account the bond between the concrete and reinforcements. It has a value of 0.8 for a good bond, and 1.6 for poor bond. k_2 considers the tensile gradient within the cross-section. This has a value of 0.5 for pure bending. k_3 and k_4 have been determined by calibration with experiments, and take into account the concrete cover and bond.

$$k_1 = 0.8 \tag{6.8}$$
$$k_2 = 0.5 \tag{6.9}$$
$$k_3 = 3.4 \tag{6.10}$$
$$k_4 = 0.425 \tag{6.11}$$

ϕ is the diameter of the steel bars, while ρ_{eff} is the effective ratio between the reinforcements and concrete in the tensile zone. The calculations can be seen in the following equations, with figure 6.14 giving background information.

$$b_{c_{eff}} = b = 200mm \tag{6.12}$$
$$h_{c_{eff}} = min(r_y + 5 * \phi; 10 * \phi; 3.5 * r_y) + s_y = r_y + 5 * \phi = 25 + 50 = 75mm \tag{6.13}$$
$$A_{c_{eff}} = 200 * 75 = 15 * 10^3 mm^2 \tag{6.14}$$
$$A_s = 3 * \frac{1}{4} * \pi * d^2 = 3 * \frac{1}{4} * \pi * 10^2 = 235.6mm^2 \tag{6.15}$$
$$\rho_{s_{eff}} = \frac{A_s}{A_{c_{eff}}} = 0.0157 \tag{6.16}$$

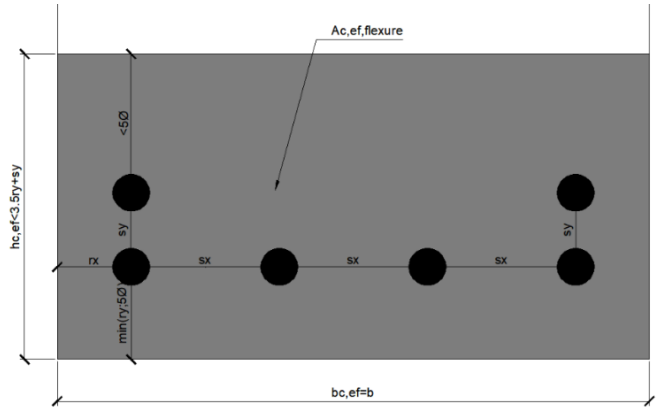

Figure 6.14: Effective area of concrete tensile zone

This all together gives an expected maximum crack spacing given in equation 6.17.

$$S_{r_{max}} = 3.4 * 20 + 0.8 * 0.5 * 0.425 * \frac{10}{0.0157} = 176.3mm \tag{6.17}$$

6.8 Water absorption test

The last test will use the water absorption capacity of concrete to determine the porosity. This is important for the ingress of fluids and gasses into the concrete that might damage the structural integrity.

Method

To analyse the porosity of the concretes, the specimen used in measuring the shrinkage be used. These specimen will be put in an oven at 75°C for one day. Once the free moisture has been removed, the weight will be measured. After that, the concrete will be left in water for two days like can be seen in figure 6.15, and weighted once more. The change in mass will come from the water retained inside the concrete, which means its volume can be determined. The calculations will be performed according to chapter 7.7.

Figure 6.15: Absorption test setup

Expected results
The mixture was designed for a porosity of 5%. The expectations are that the CEM I mixture will fall slightly above that due to the poor curing conditions. The CEM III mixture is expected to be more porous than CEM I.

7 Experimental results

This chapter will present the results from the experiments discussed in chapter 6.

7.1 Shrinkage test

The tables of all shrinkage results can be found in Appendix A. Figures 7.1a and 7.1b show the total shrinkage of three specimen. The CEM I specimen show shrinkage curves that are quite close together. In the first few days the specimen swell with 40 microstrain. This is approximately 15% of the total shrinkage. After these days, the concrete starts shrinking. The first 10 days account for half of the total shrinkage, after which it starts to slow down. After 50 days the shrinkage becomes almost negligible. The end results after 75 days are 257, 267 and 282 microstrain.

The CEM III concrete shows slightly more spread between the three specimen. The swelling can not be seen in this curve, due to the measuring days being different for CEM III. When looking at the curves it quite clear however that some swelling has taken place. Most of the shrinkage can again be found within the first 10 days after casting, but it slows down less compared to CEM I. The end results after 73 days are 324, 290 and 297 microstrain.

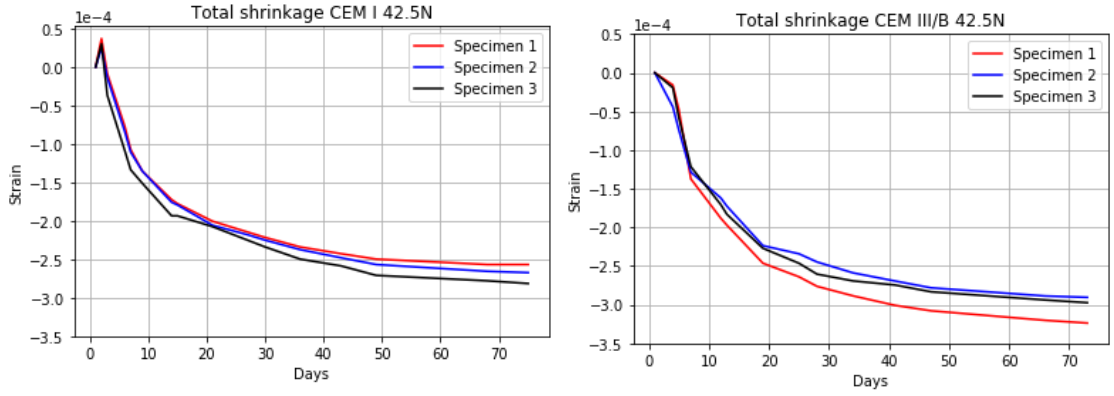

(a) CEM I 42.5N **(b)** CEM III/B 42.5N

Figure 7.1: Total shrinkage of three specimen over a 75 day period. The CEM III/B specimen experience a 13% additional strain compared to CEM I.

Figure 7.2a and 7.2b represent the autogenous shrinkage of the wrapped concrete specimen. Again, the swelling becomes really evident when looking at the graphs. The shrinkage from both CEM I and CEM III seem to follow an exponential curve. The CEM III shrinks significantly faster however, at double the pace. At the end of the 75 days of measuring, the CEM I specimen have shrunk with 70, 79 and 70 microstrain. The CEM III specimen have shrunk with 130, 127 and 135 microstrain. All samples were still experiencing shrinkage in the last days of measuring.

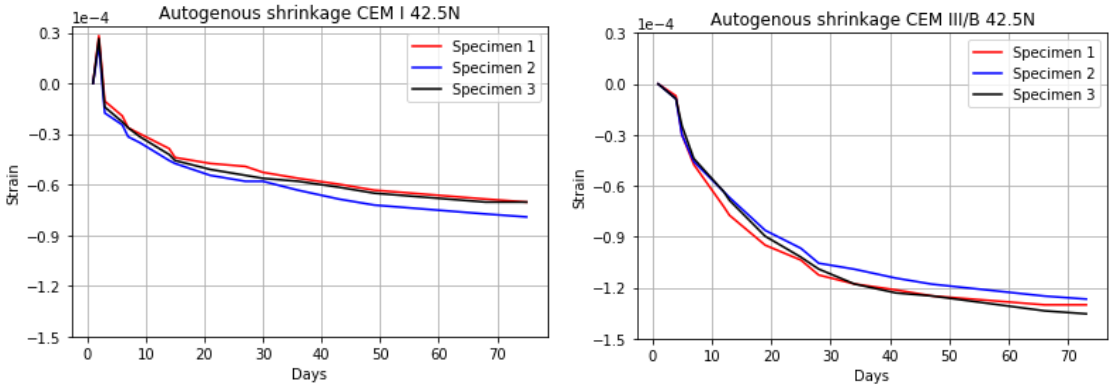

(a) CEM I 42.5N **(b)** CEM III/B 42.5N

Figure 7.2: Autogenous shrinkage of three specimen over a 75 day period. The CEM III/B specimen experience nearly double the strain, and shrink faster in the last testing weeks.

By subtracting the autogenous shrinkage results from the total shrinkage, the drying shrinkage results from figures 7.3a and 7.3b are obtained. The end results are strains of 187, 188 and 211 microstrain for CEM I samples, and 194, 164 and 162 microstrain for CEM III samples.

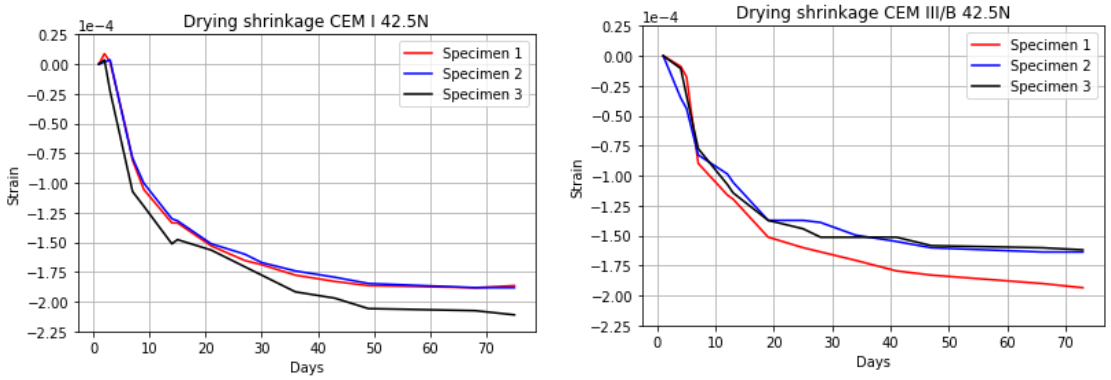

(a) CEM I 42.5N **(b)** CEM III/B 42.5N

Figure 7.3: Drying shrinkage of three specimen over a 75 day period, achieved by subtracting the autogenous shrinkage from the total shrinkage. CEM I has 13% more drying shrinkage.

The mean values of the above results are used to form figure 7.4a and 7.4b. The dotted lines represent the autogenous shrinkage, with the solid lines representing the total shrinkage. The distance in between signifies the drying. The end values for the shrinkage can be found in table 7.1.

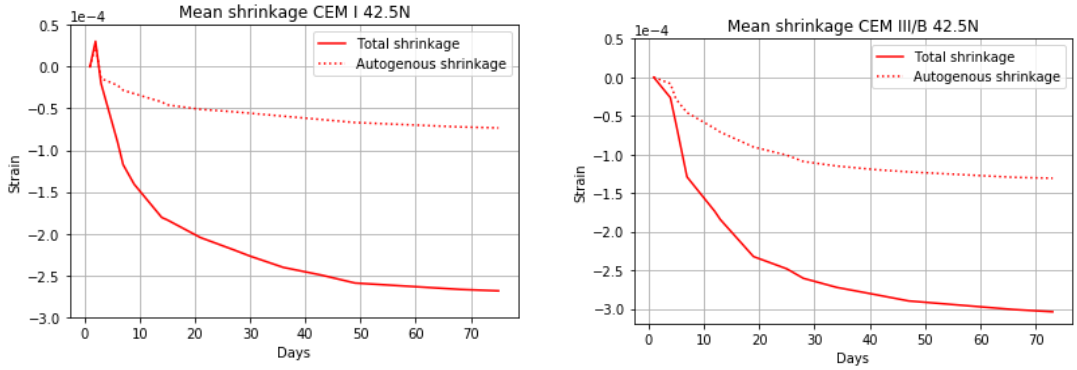

(a) CEM I 42.5N **(b)** CEM III/B 42.5N

Figure 7.4: Mean total shrinkage of the three specimen over a 75 day period. The differences between the autogenous and total shrinkage denote the drying.

Shrinkage type	CEM I shrinkage microstrain	CEM III shrinkage microstrain	**Difference CEM I/CEM III**
Total	268	304	-12%
Autogenous	73	131	-44%
Drying	195	173	13%

Table 7.1: Mean results shrinkage test

Since shrinkage depends on the water movement within the concrete, the water loss of all specimen is given in figures 7.5a, 7.5b, 7.6a and 7.6b. The water loss from the drying shrinkage mainly comes within the first three days. After this, the water loss slows down significantly. The autogenous shrinkage specimen also show a water loss, even though no water should be lost when wrapped with the sealing tape. The water loss remains pretty constant even after over 70 days.

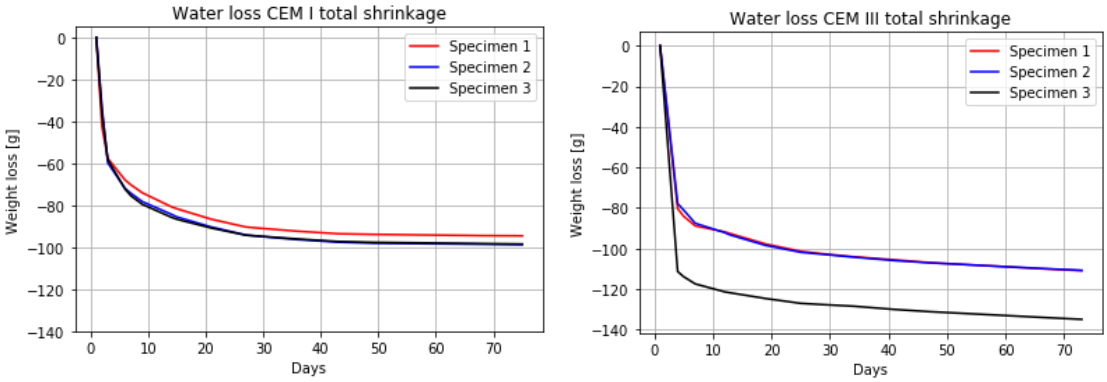

(a) CEM I 42.5N **(b)** CEM III/B 42.5N

Figure 7.5: Water loss due to total shrinkage of three specimen over a 75 day period. CEM III/B loses more water and has a higher variance for the three samples.

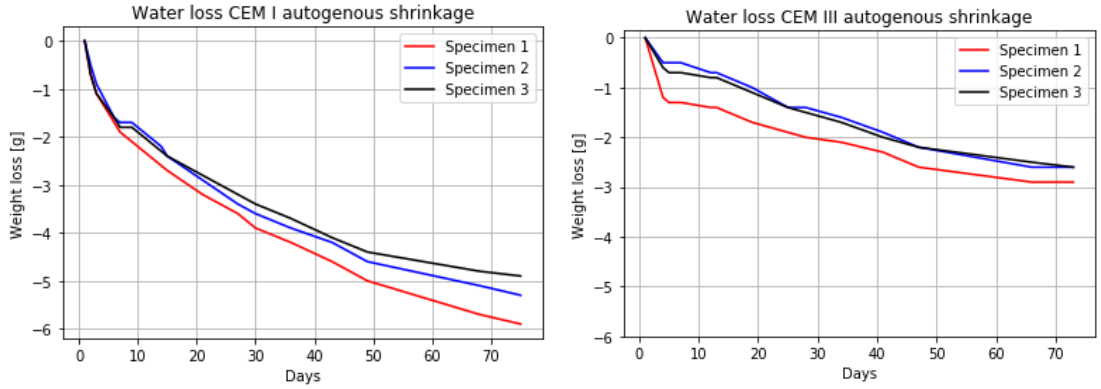

(a) CEM I 42.5N **(b)** CEM III/B 42.5N

Figure 7.6: Water loss due to autogenous shrinkage of three specimen over a 75 day period. The weight loss is insignificant for both samples compared to the total water loss.

The mean water losses can be seen in figure 7.7. Table 7.2 shows the differences in a table. Especially the autogenous shrinkage specimen show a considerable difference in water loss between CEM I and CEM III. However when looking at the total weight, this loss becomes insignificant.

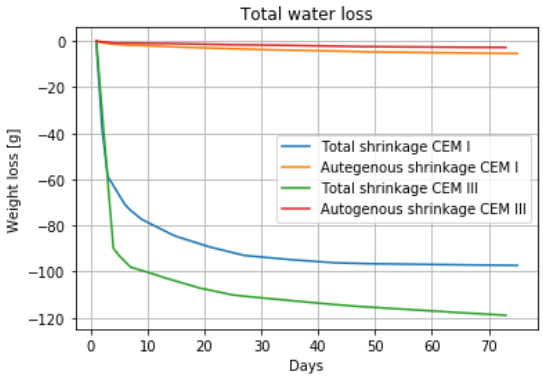

Figure 7.7: Mean total water loss of the three specimen over a 75 day period.

Shrinkage type	CEM I shrinkage water loss [g]	CEM III shrinkage water loss [g]	**Difference CEM I/CEM III**
Total	97.3	118.9	-18%
Autogenous	5.4	2.7	100%

Table 7.2: Mean results water loss

7.2 Compression test

The results of each individual cube compression test can be found in Appendix A. Figure 7.8 shows the mean values of each day of compression tests, including the standard deviation. The 97% humidity cured cubes all surpass the 50MPa compressive strength at 28 days, with the CEM I mixture reaching 53.70MPa and the CEM III reaching 54.10MPa. the CEM I gains 70% of its strength within the first three days, while the CEM III mixture gains most of its strength after these three days.

The 55% relative humidity cured cubes show a much bigger difference. At 28 days, the cubes reach an average strength of 50.27MPa and 36.45MPa. The final strength at 56 days is 53.10MPa and 39.85MPa. The CEM I does not show a drastic difference in strength for the two different curing conditions, unlike the CEM III concrete with a difference of nearly 50%. The standard deviations between the cubes on each day is also significantly higher for these specimen for both the CEM I and CEM III mixtures. The end results after 28 days can be seen in table 7.3.

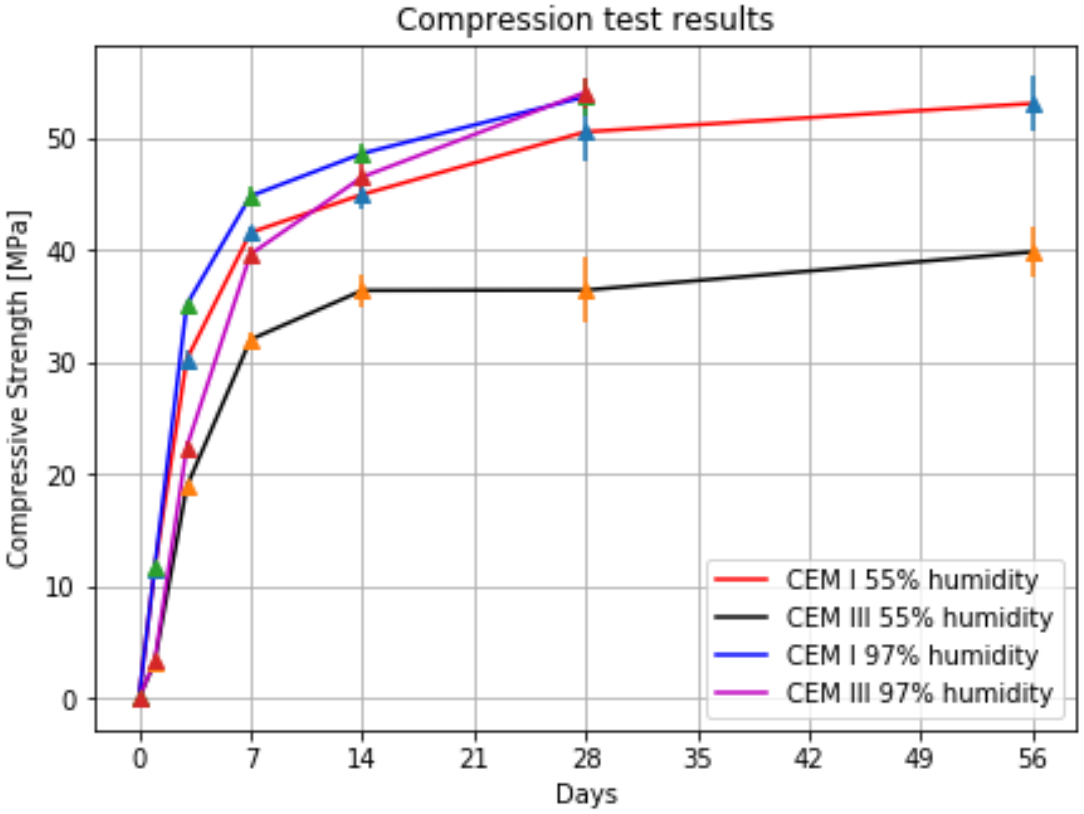

Figure 7.8: Compression test results with mean values and std. The lower relative humidity especially impacts the strength gain of CEM III/B. The variances for the 55% humidity cured cubes are significantly higher.

Relative Humidity	CEM I compressive strength [MPa]	CEM III compressive strength [MPa]	**Difference CEM I/CEM III**
55% 97%	50.27 53.70	36.45 54.10	38% -1%
Difference [97%/55%]	7%	48%	-

Table 7.3: Final results compressive strength at 28 days

7.3 Static modulus test

The static modulus tests give the results given in figures 7.9a and 7.9b. It is quite noticeable that the compressive strength in these tests are significantly lower than the strength of the cubes of chapter 7.2. Both specimen have half the strength of the cubes, with CEM I reaching nearly 24MPa and CEM III reaching 17MPa.

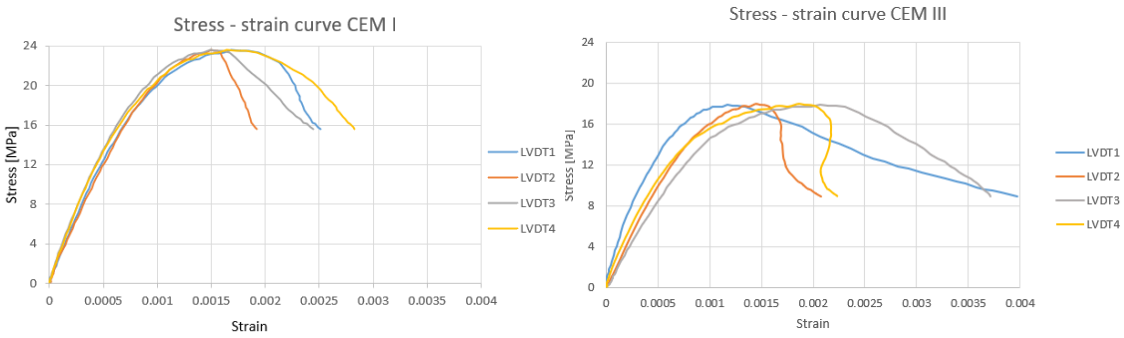

(a) CEM I 42.5N **(b)** CEM III/B 42.5N

Figure 7.9: Stress - strain curve for static modulus test, where an LVDT is placed on every side of the specimen. CEM III/B concrete experiences much more localised deformations and brittle failure.

The Young's modulus is determined by the slope of the linear part of the stress-strain curves. The CEM I LVDT's remain quite close together, and give an average E-modulus of **33GPa**. The LVDT's attached to the CEM III specimen experience a larger difference in the measurements, with an average E-modulus of **28GPa**.

After the peak strength has been reached, both mixes soften. The CEM I concrete fails quasi-brittle, with all four sides still maintaining its stiffness during the unloading. Due to the machine being stopped early, not the full softening and final strain can be measured.

The CEM III mixture again experiences a significantly higher variance between the LVDT's. Two LVDT's show softening, shown by the blue and grey line in the graph. The orange line shows very brittle behaviour, and the yellow line even shows snapback. The brittle behaviour was also very visible during the test, since the corners were spalling. For this test the machine has been stopped at a later point, so that more of the softening can be visualised. The specimen fails at a maximum of 0.004 strain.

7.4 Workability test

The workability test for this thesis is a visual inspection. The expected and also wanted result, is that all the aggregates are covered by a layer of cement paste. Figure 7.10 shows that this is indeed the case.

Figure 7.10: Visual inspection of the consistency of fresh concrete

7.5 Unreinforced three-point bending test

The three point bending tests give a multitude of results. The Young's modulus in tension, maximum tensile strength and fracture energy can all be extracted from these results. The crack propagation of both tests can be seen in figures 7.11a and 7.11b. Since the crack is hard to see after unloading, a black marker is drawn to indicate the crack path.

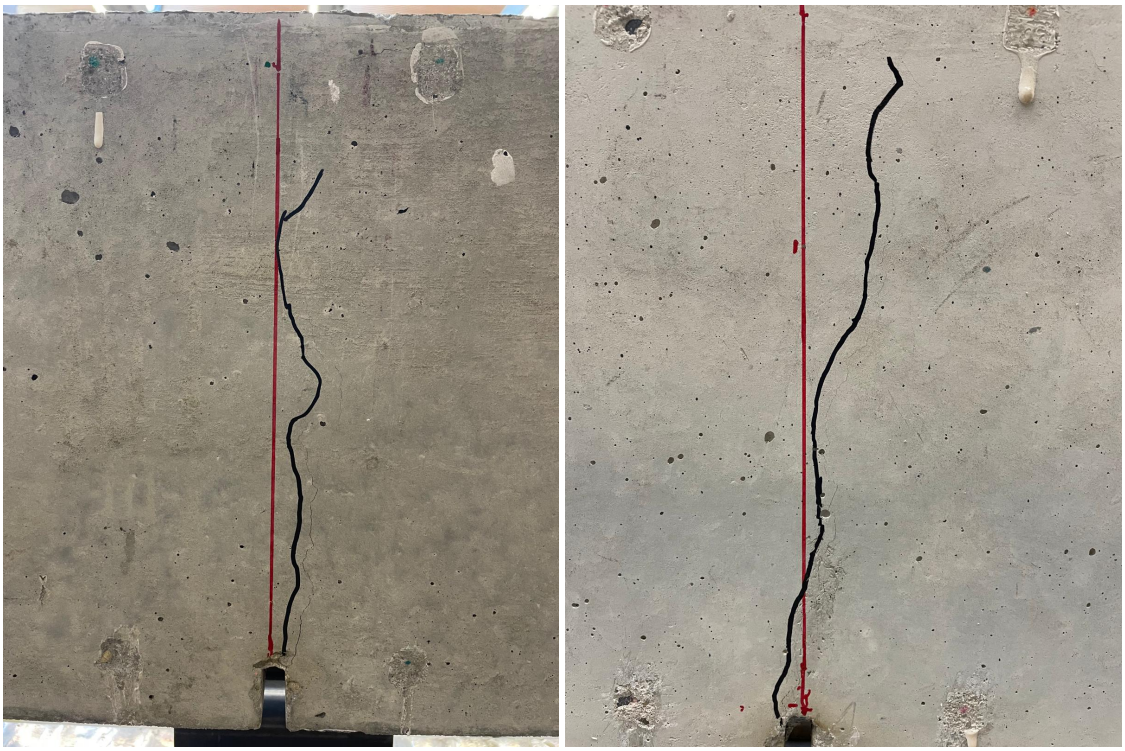

(a) CEM I **(b)** CEM III

Figure 7.11: Cracks of three-point bending test

Figures 7.12a and 7.12b show the relation between the stress at the notch and the displacement of the crack mouth opening. The maximum tensile stress of the CEM I beam is 3.40MPa, and 2.81MPa for the CEM III beam. The test is stopped at a crack width of 0.5mm for both specimen, since otherwise the likelihood of total collapse of the beam was too high.

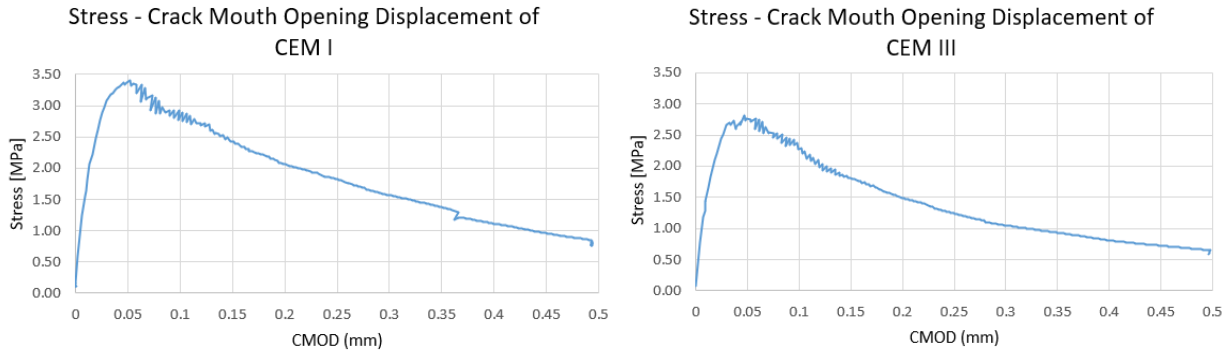

(a) CEM I **(b)** CEM III

Figure 7.12: Tensile stress - CMOD curve. The tensile stress for CEM I concrete is 21% higher, with slower softening especially right after the peak.

In figure 7.13a and 7.13b the relation between the vertical displacement and force is shown. According to the method described in chapter 6.6, the Young's modulus can be extracted. This results in an E-modulus of 38GPa and 31GPa for CEM I and CEM III consequently. The fracture energy can be extracted according to chapter 4.5. The total energy used for the fracture is extracted by calculating the area underneath the force - displacement curve. This is divided by the total area where the crack occurs. Since it is tricky to find the exact location where the crack ends, the full height of the beam is used as the crack height. This is not too far off the reality. The results are given in equations 7.1 to 7.5. The final results can be found in table 7.4.

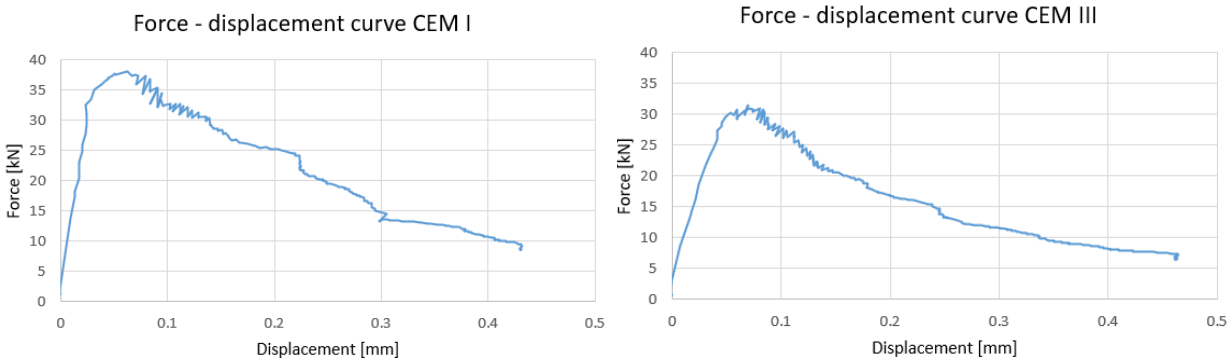

(a) CEM I **(b)** CEM III

Figure 7.13: Force - vertical displacement curve

$$A_{crack} = b * h = 200 * 290 = 58 * 10^3 mm^2 \tag{7.1}$$

$$W_{CEMI} = 12.1 * 10^3 Nmm \tag{7.2}$$

$$W_{CEMIII} = 8.84 * 10^3 Nmm \tag{7.3}$$

$$G_{f,CEMI} = \frac{W_{CEMI}}{A_{crack}} = 0.209 N/mm = 209 N/m \tag{7.4}$$

$$G_{f,CEMIII} = \frac{W_{CEMIII}}{A_{crack}} = 0.152 N/mm = 152 N/m \tag{7.5}$$

Property	CEM I	CEM III	**Difference CEM I/CEM III**
Tensile strength	3.40MPa	2.81MPa	21%
Young's modulus	38GPa	31GPa	13%
Fracture energy G_f	209N/m	152N/m	38%

Table 7.4: Final results tensile strength at 28 days

For all the curves some noise can also be seen right after the peak has been reached.

7.6 Reinforced four-point bending test

The results from the four-point bending test can be seen in figures 7.14a and 7.14b. Due to the poor visibility of the cracks after unloading, the crack patterns have been drawn with a black marker. The spacing of the cracks have been noted in table 7.5. It is notable that the CEM III/B specimen has a total of nine cracks, with the CEM I only having seven cracks. The total spacing of the cracks comes to 1m for the CEM I mixtures, which exactly coincides with the spacing of the loads. That means that all cracks can be found in the length where the moment is maximal. The CEM III/B mixture however has cracks spanning 1.2m. This means that some cracks are found in places where the moment is not maximal.

(a) CEM I **(b)** CEM III

Figure 7.14: Cracks of four-point bending test with spacing indicated

	Concrete using CEM I 42.5N	Concrete using CEM III/B 42.5N
Cracks spacing number	Crack spacing [mm]	Crack spacing [mm]
1	213	175
2	180	148
3	164	151
4	173	198
5	128	99
6	160	190
7	-	100
8	-	147
Average	170	151
Max	213	198

Table 7.5: Crack spacing

7.7 Water absorption test

The water absorption test results can be found in table 7.6. The calculations can be found in Appendix A.3. The porosity is significantly higher than expected.

CEM I porosity	CEM III porosity	**Difference CEM I/CEM III**
8.46%	9.64%	-13%

Table 7.6: Final results porosity after 75 days

8 Life-cycle effects for a building

The experimental results show that the sub-optimal curing conditions can have a high impact on the material and mechanical properties. These properties in turn affect the durability of a building. A lower durability then results in more maintenance or even a lower service life of a structure, influencing the practicality and sustainability of the building. This chapter will compare the life-cycle effects of the two different concrete mixes, based on literature research and results. The life-cycle is shown in figure 8.1. The transport will not be taken into account.

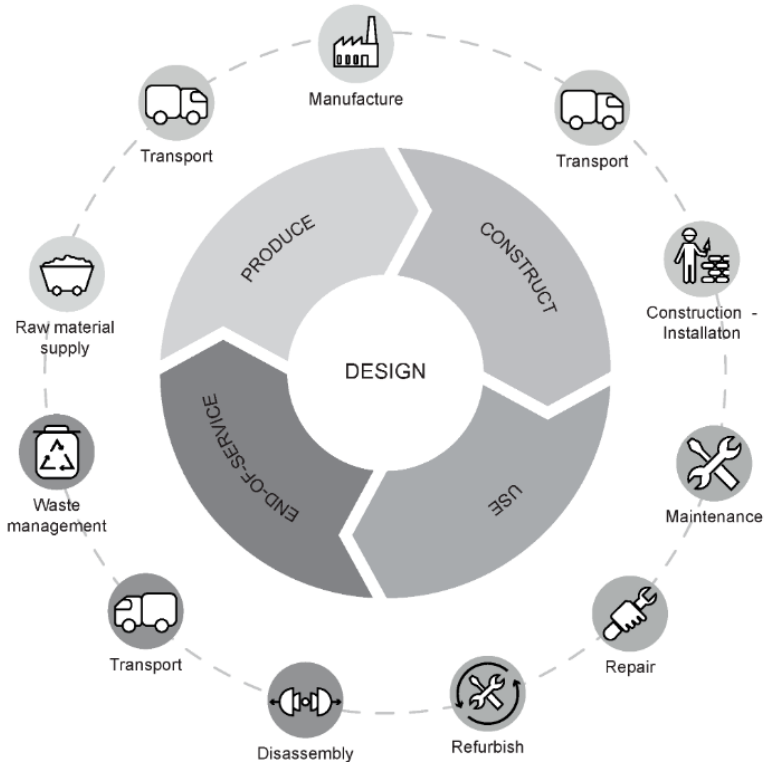

Figure 8.1: Life cycle of a building [98]

8.1 Sustainability of the production process

The first factor influencing the sustainability, is simply the production process of the two different kinds of cement. Like stated in chapter 2.1.1, clinker is produced by grinding and heating calcareous and argillaceous materials into a fine blend. This process takes a lot of energy and produces quite some CO_2. This is for two main reasons: The thermochemical reaction of limestone produces a lot of CO_2, and the necessary fuel for achieving such high temperatures does the same. In Europe it comes down to a total of 839kg of CO_2 per ton of clinker produced [92].

For ground granulated BFS it might be stated that it is a waste product of the steel manufacturing, thus it has 0 emissions. This is false however, since this slag can not be used immediately for cement. The process of drying and grinding this slag into a fine product emits 130kg of CO_2 per ton of GGBFS [94].

Using this information, the production of CEM I and CEM III/B can be compared. Assuming no other constituents are put into the cement mix, CEM I will contain 100% clinker and CEM III between 66-80%. A lower value of 70% is assumed in the scenario. This gives the results given in table 8.1.

Cement type	Clinker percentage	Clinker emission in [kg CO_2/t]	GGBFS percentage	Clinker emission in [kg CO_2/t]	Total emission in [kg CO_2/t]
CEM I	100%	839	0%	130	839
CEM III/B	30%	839	70%	130	342

Table 8.1: CO_2 costs for production of CEM I and CEM III/B

8.2 Effects on construction process

The construction process will also be impacted by the different cements, mainly due to the speed at which builders can continue with every stage. If a building is being made with several floors cast in situ, the floor needs to hydrate a while to obtain substantial strength, before any construction workers and machines are allowed on it. According to the practical experience at Pieters Bouwtechniek and other sources, about seven days are required before allowing heavy machinery on this floor [93]. This is the point where the concrete reaches about 70% of its strength. In the case of the specimen tested in this Thesis, after one week already 80% of the final strength was reached for CEM I. This strength was also more than the 42.5MPa characteristic strength that is used in calculations in the Eurocode. In the poor curing conditions, only 50% of the final strength was reached for the CEM III concrete however. And on top of that, the final strength did not even reach 42.5MPa. Depending on the design of the structure, this could make the building site very dangerous for the workers and even cause collapse. If the machinery used come close to the allowable loads, the structure might deform too much and even fail.

If 70% of the 42.5MPa compressive strength should be reached before continuing the build, a minimum wait of 28 days is necessary according to the results in figure 7.8. This means that per floor in a building, it would take four times as long when using CEM III/B to continue compared to CEM I. This does not necessarily impact the sustainability that much, since none of the machinery would need to be used during the waiting period. It does however increase the costs and manufacturing time tremendously.

Another likelihood is that more cracks appear in a CEM III concrete during construction. Most concrete elements will experience some form of tension during construction. With the CEM III mixture gaining its strength so late, it is expected that the difference in

fracture energy will be even greater at this stage than after 28 days. A lower fracture energy results in cracks propagating easier and thus more and larger cracks.

8.3 Effects on service life

For the service life both the durability and maintenance requirements are important factors. It is hard to define real numbers to the difference in service life between the two concrete mixtures, since it all depends on the loads, kinds of elements, connections and more. This means that the following explanations will be slightly subjective, but still based on actual facts and data.

The first factor tremendously impacting the service life, is the combination of the higher porosity and lower fracture energy. Due to the link between porosity and permeability, porous concrete allows for chlorides to ingress, which can affect the durability of the reinforcements. This in combination with the lower fracture energy, means that larger and thicker cracks are formed. This again leads to chlorides to penetrate the concrete faster. To combat this chloride ingress, much more maintenance would be required when applying CEM III/B concrete. Chloride ingress damages the strength and durability of the steel, which is necessary for the safety of a structure. Regular maintenance results in both higher costs and an unsafe feeling for the people utilizing the building.

A higher porosity also results into more moss grow in the concrete, like the CROW organisation analysed after massive moss grow was found in their high speed line [100]. This affects both the weight, integrity and aesthetics of the concrete.

Another factor affecting the service life, is the shrinkage. Like is stated in chapter 3.1, shrinkage in elements that are free to deform does not warrant any worry. But in buildings elements are often restrained in movement. If the elements are restrained from moving but want to deform due to shrinkage, additional tensile stresses will be present, once again causing more cracks to occur.

The Young's modulus will also affect the service life. Since the CEM III/B concrete gives lower E-moduli in both compression and tension, the deformations will be larger as well. Since there are certain requirements for the allowable deformations in a structure, either the strength or the dimensions of the concrete elements would need to increase.

Finally, the high variance in the CEM III gives worries for the overall safety of a structure. A structure is only as strong as its weakest link. A high variance, especially in combination with the already weaker mechanical properties, results in large insecurities on the overall integrity of the building. When putting together all the negative effects on the service life that CEM III gives compared to CEM I in sub-optimal curing conditions, it can be stated that CEM III concretes would require more maintenance and have a lower durability. This will all surely affect the sustainability, costs, and safety of the building.

8.4 Recycling

The last phase of the life-cycle of a building comes when the building is demolished. Some materials become landfill or are down-cycled, which is of course disadvantageous for the sustainability. With the foresight of recycling, up-cycling or even reusing more and more material to achieve the sustainability goals in 2050, the want for recycling concrete increases as well. Some concrete is already being recycled, to gain back the aggregates and fine cement [101]. When comparing CEM I and CEM III, no large differences are expected for recycling. However, the sustainable gain in recycling CEM I might be slightly higher, due to a larger amount of clinker being present. It is still not feasible to recycle concrete in mass though, due to the enormous amount of required energy to extract the aggregates and especially cement.

9 Discussion

This chapter will discuss the findings of this report. First the results of the experiments will be explained, which is followed by a discussion on the life-cycle of a building.

9.1 Experimental results

Shrinkage
The drying shrinkage from the CEM I specimen is slightly higher in the first few months. This was an unexpected result according to the literature study of chapter 4.1.2 since CEM I hydrates faster, which would result in less free water being available. However in many cases, the evaporation of free water actually does not contribute to shrinkage. Shrinkage is mainly caused by internal stresses, which in turn are caused by the loss of adsorbed water or water in small voids. The fast hydration of CEM I contributes to these small voids and adsorbed water being created earlier, so it will be prone to shrinkage faster as well.

The autogenous shrinkage specimen consistently lose a small amount of weight, which means that they are also susceptible to drying shrinkage. This can be explained by the small areas which are not covered on the top and bottom of the specimen. This can affect the results of the autogenous shrinkage. Especially after 30 days it is not expected that the autogenous shrinkage keeps going at the same consistent rate for both CEM I and CEM III. There is a high likelihood that a small portion of this shrinkage is due to the drying. There is also quite a large difference percentage wise between the CEM I and CEM III water loss for these samples. This can be explained by the learning curve of wrapping the specimen in the sealing tape. The CEM I samples were cast earlier and wrapped less neatly. The CEM III concrete was wrapped more neatly.

The autogenous shrinkage of CEM III concrete is nearly double that of CEM I concrete. This is in line with the expectations of chapter 4.1.3. It can be explained by looking at the pore structure of CEM III concrete. Due to the Blast Furnace Slag, the pore size decreases and the discontinuities increase. Due to these discontinuities occurring, capillary water gets sucked into small voids, thus creating local compressive stresses. In other words; Autogenous shrinkage.

The total shrinkage seems much lower compared to shrinkage of moist cured specimen. This is probably due to most of the moisture loss being free water, which does not affect shrinkage, like stated in chapter 3.4. It does mean that there is less water available in a later stage for the cement to react with. This also becomes evident when looking at the compression tests of CEM III. Due to less water being available for the reaction, the compressive strength is significantly lower than it is supposed to be.

The total shrinkage of CEM III/B is only 12% higher than the CEM I shrinkage, which does not seem all too bad. It does seem that the CEM III specimen were experiencing more shrinkage in the last weeks of testing compared to the CEM I. This means that the

testing has probably stopped too soon to see the long term effects. Unfortunately this can not be helped due to the allocated time of this Thesis. It is likely that the shrinkage of CEM III concrete would continue more rapidly if being tested for a longer period of time.

Compression test
The compressive strength of most of the samples are as expected in chapter 6.3, except for the CEM III cubes cured in 55% relative humidity. It was expected that an average strength of 45MPa would be reached after 28 days, but only 36MPa was achieved. This is 27% less than the 50MPa that the CEM III/B samples achieve, and not even the 42.5MPa that the compressive strength should be at minimum. This can be explained by the poor hydration circumstances. Like chapter 3 indicates, the relative humidity has a great influence on the hydration process. For CEM III this effect is larger, due to its mineralogical composition. The BFS needs calcium oxide (CH) to react, which is made by the reaction of C_3S and C_2S. It thus takes more time for this chemical reaction to take place, which means there is a larger volume of unreacted water at the beginning. Due to the low relative humidity during hydration, this water evaporates leaving a larger volume of pores in the concrete. From this point it's a simple equation: More pores equal less material equals a lower strength.

When comparing these results to the 97% relative humidity cured cubes, the results do not seem strange at all. It can be seen in the results of the water loss in chapter 7.1, that most of the water is lost within the first three days. This is also the time that CEM I concrete gains 70% of its strength. It thus makes sense that the sub-optimally cured and moist cured cubes do not differ too much in strength, with only a 7% difference. CEM III/B however, gains most of its strength after these three days. When comparing the curves seen in figure 7.8, it can be seen that the first three days give quite similar results for all CEM III/B samples. However due to poor hydration, the 55% cured cubes are not able to gain as much strength later on, since there has been a major water loss already.

The moist cured cubes achieve expected results, with a 28-day strength of between 50-55MPa. The CEM III/B cubes are 1% stronger, which is a negligible difference.

The standard deviations of the poorly hydrated cubes is significantly larger, which again can be seen in figure 7.8. This is especially the case in the later stages of testing. This can be explained by the localisation of imperfections, leading to failure. Like stated before, the poor hydration circumstances lead to more pores in the concrete. If these pores localize, the concrete becomes especially weak in one area. This can lead to failure occurring sooner. If the pores are spread out more, the concrete becomes more homogeneous and will probably be stronger.

Static modulus test
The first thing to notice, is that none of the specimen come close to the compressive strength of the cube compression test. The maximum strength they reach is about half

the cube strength. This can be explained by the size of the samples. A material can be seen as a chain of links connected to each other. Global failure occurs, when the weakest link is broken [87]. This is why size effect is so important for concrete, since it is susceptible to imperfections. The size of the samples used in the static modulus test are 284mm in height, compared to the 150mm of the cubes which are about half the height.

The second interesting note, is the large difference in strain for especially the CEM III sample. Two of the sides experience very brittle failure and even snapback, while the other two sides remain pretty much intact. This can again be explained by the localisation of the pores. During the entire hydration process, these specimen have been put onto a cabinet. This means that one side of the concrete was always in direct contact with the cabinet, while the other three sides were exposed to the air. It is very likely that the most exposed sides also experienced the most water loss, and thus are more porous. This immediately explains the large difference in Young's modulus on each side of the CEM III specimen as well. Like stated before, due to the fast development of strength of clinker, the CEM I concrete is affected less intensely.

The goal of this test was to find the Young's modulus. A difference of 18% can be found between the 33GPa for CEM I and 28GPa of CEM III. The expectation according to the Eurocode calculations of chapter 6.4, were 35GPa and 33GPa, which means especially the later is quite different. These predictions were made using the Eurocode, where the compressive strength gives a prediction of the Young's modulus, since these characteristics are connected. The characteristic strengths of the concrete were assumed to be 50MPa and 45MPa. It turns out however, that the mean strengths were 50MPa and 36MPa. Converting these mean strengths into characteristic strengths, 1.64 times the standard deviation should be subtracted according to the Eurocode [88]. This gives a result of consequently 47.5MPa and 31.6MPa. This gives expected Young's moduli of 34GPa and 31GPa according to the Eurocode, which is not too far off the actual result for CEM I. The CEM III still has a larger difference, which can be explained by the higher porosity. The Eurocode accounts for a well-mixed and well-hydrated concrete, which now is not the case.

The last noticeable point, is the snap-back behaviour with the softening of CEM III. This means that more energy is released than the material can absorb. The energy release can be explained by the localised failure. One side of the concrete fails, which means the energy exerted on this side is released suddenly. Since this side has failed, the material can hardly absorb any energy. This causes the so-called snapback [85].

Three-point bending test

The results from the maximum tensile stress are very much in line with the theory explained in chapter 7.5. With an expected tensile strain of 100 microstrain, a linear relationship is found between the Young's modulus and stress. With 33GPa and 28GPa as results for the Young's modulus from the static modulus test, tensile stresses of

3.3MPa and 2.8MPa would follow. The actual results are 3.40 and 2.81MPa. This 21% difference can again be explained by the porosity of the blast furnace slag cement concrete.

However, the three-point bending test gives an E-modulus of 38GPa and 31GPa for CEM I and CEM III/B consecutively. This is 10-15% higher than the E-modulus extracted from the static modulus test. This is counter-intuitive, since the theory from chapter 4.2 suggests the Young's modulus in compression should be slightly higher. A likely cause for higher values in the three-point bending test, is the speed of the test. The peak stress in this test is reached in 10 seconds, while the static modulus test needed over a minute to reach the peak. According to multiple studies, the Young's modulus becomes higher if the strain rate increases [89] [90]. Concrete is a viscoelastic material, meaning the deformation depends on both the applied load and the rate it is applied with [91]. At a higher strain rate the concrete has less time to undergo deformation, which leads to a higher E-modulus. Another reason might be the crude approximation of the formula used to determine the E-moduli.

The fracture energy of the CEM I mixture is 38% higher, which means that a lot more energy is required to crack this material. This result is due to the higher tensile strength of the material, and the more ductile softening curve compared to CEM III.

Lastly, the graphs of chapter 7.5 show that there is some noise right after the peak is reached. This can be explained by the way the test is performed. The three-point bending tests are controlled by the crack mouth opening displacement, which is measured by an LVDT underneath the beam. The speed of the crack mouth opening displacement should be 0.005mm/s, which is the displacement of the LVDT. This displacement is repeatedly signaled to the hydraulic cylinder, so that the force in the cylinder can be adjusted and the loop continues this way. Since the LVDT has to direct the cylinder, a slight delay occurs causing noise.

Four-point bending test

The maximum spacing from the experiments is larger than the maximum spacing from the prediction. This can be explained by the friction being poorer than expected, due to the curing conditions. With a higher porosity there is less material to provide friction between the concrete and steel, which impacts the bond strength. The impact of friction can be seen in formula 6.7 in chapter 6.7. Another reason can be that the effective height of the concrete in the tensile zone is higher than calculated. This zone is approximated in the Eurocode, but can be different from reality. If this tensile zone is higher, the effective steel-to-concrete ratio is lower, which increases the maximum spacing.

It is interesting to note that both the mean and maximum crack spacing is lower for the CEM III mixture. There can be multiple explanations for this phenomenon. The student has made the reinforcement cages himself by hand. There is a high likelihood of the spacing between the rebars not being consistent in the CEM I and CEM III concrete.

This affects both the concrete cover and effective tensile area of the concrete. If the proper concrete cover is not maintained everywhere but is higher, the spacing between the cracks increases as well. Another reason might be the quality of the reinforcement bars used. Not all bars are exactly the same, with some bars showing some rust or having plastic attached. Depending on how far the corrosion has gone, it might improve or weaken the bond.

Water absorption test
The last test is the water absorption test, where the volume of pores can be extracted. Both mixtures contain a larger amount of pores than the designed 5%, with 8.46% for CEM I and 9.64% for CEM III. This increase in porosity is to be expected, due to again the sub-optimal curing conditions. In a lower relative humidity, concrete is much more prone to drying which in turn leads to both shrinkage and a higher porosity.

The second observation of the test, is the 13% higher porosity for the CEM III/B mixture. This is again to be expected when looking at the hydration process and shrinkage results. Due to the late chemical reactions in CEM III, more free water is available in the first days after casting. This results in a higher water loss in a low humidity, and thus more pores.

Link between properties
When comparing the mechanical properties of the CEM I and CEM III concretes in a 55% relative humidity, it becomes evident that CEM III is affected more negatively for all properties. This can be explained by the link between all the properties. Due to the mineralogical composition of the CEM III/B 42.5N cement, the curing in 55% relative humidity causes a greater porosity compared to CEM I 42.5N. In the pores of the CEM III mixture, more free water is available since the hydration is slower. The movement of this free water in small capillary pores causes shrinkage, thus explaining the increased shrinkage. The increased porosity means that there is less solid material available to provide resistance and strength. Thus, the decreased compressive strength, tensile strength and Young's modulus seem logical. A higher porosity also results in a more brittle behaviour and a larger uncertainty, since there are more imperfections in the material.

9.2 Life-cycle of a building

Chapter 8 demonstrates how the different material and mechanical properties might influence the life-cycle of a building. The production process of CEM I emits nearly three times as much kilograms of CO_2 per ton of cement produced, compared to CEM III/B. This is mainly due to the production of clinker using so much energy to grind and heat up the raw materials. CEM III uses a large percentage of blast furnace slag, which is a waste product of the steel production industry. This slag only needs to be grinded, costing much less energy to produce. It can however be argued, that producing blast furnace slag is more detrimental than believed. More and more alternative solutions are

brought in the production of steel, like for example the use of an electrical furnace. This lowers the carbon footprint of the production of steel, but also gives slag with different properties [102].

The construction process when using poorly cured CEM III is impacted much more. Due to the already slower strength gain of CEM III, the addition of the poor curing conditions limits how much strength it can gain later on as well. For the safety of the construction it thus makes sense that the costs and time for producing a building are increased. Minimum strength requirements are set for continuing with the build, for the overall safety.

The service life is also impacted by the difference in mechanical strength that CEM III has on the building site. More maintenance will be required, and the durability of the structure will be lower. This makes sense, since all the mechanical properties are worse than those of CEM I.

Recycling was analysed at last, where it was stated that both CEM I and CEM III concrete should have similar recycling stages. Both materials would need to be crushed to extract the aggregates and cement. Clinker is worth more than blast furnace slag however, when looking at the environmental impact. It thus makes sense that the gain in recycling CEM I would be higher than recycling CEM III.

Part III:
Conclusions and recommendations

10 Conclusion

Due to the ever-growing demand for sustainable building solutions, concretes with a lower carbon footprint are being advocated more often. Since clinker is the largest contributor to unsustainable concretes, large parts in cement are being replaced with waste-products of other industries. One of these products comes from the manufacturing of steel with a blast furnace, called blast furnace slag. This thesis has been comparing the mechanical properties and life-cycle effects in buildings, of two different concrete mixes: A regular Portland cement concrete using 95%-100% of clinker, and a CEM III/B concrete replacing 66-80% of the clinker with blast furnace slag. Even though CEM III/B has been positively applicable in maritime structures for a while now, the conditions above sea-level heavily influence the mechanical properties. For this reason the CEM I and CEM III/B concrete mixes have been compared to each other by experiments under sub-optimal curing conditions. Instead of the 97% relative humidity curing chamber which the lab often uses for concrete tests, a 55% relative humidity chamber has been used. This simulates the conditions of the Dutch building site around summer, or when the wind speeds are very high.

The **first research question** that has been answered is as follows:

What are the differences in mechanical properties for a CEM I 42.5N and CEM III/B 42.5N concrete mixture, when cured in a relative humidity of 55%?

To answer this question, some literature research was first conducted to explain how the hydration process works for the two different cements. This research suggested that the hydration process of CEM III is much slower, due to the mineralogical composition. The BFS needs CH to hydrate, which comes from other reactions. After the hydration, the mechanical properties of concrete were studied, so that the experiments could be conducted properly.

The shrinkage tests suggested that the total shrinkage after 75 days of CEM III/B concrete is 12% higher than of CEM I concrete. This is mainly due to the autogenous shrinkage being double, since the drying shrinkage is 13% lower. The water loss of the BFS concrete is 18%, resulting in a more porous concrete. The CEM III specimen were still losing more water and shrinking more in the last weeks of the experiments. When a longer period of time would have been used for testing the shrinkage, it is likely that the differences would have been bigger.

The compression tests showed that the CEM III/B mixture reaches only 62% of the strength of the CEM I concrete. It only achieved a strength of 36.45MPa, while the CEM I achieved 50.27MPa after 28 days. Due to the hydration process for CEM III/B becoming more active after one week, there was a large difference in compressive strength within the first week. However due to the water loss, the BFS concrete could not hydrate

optimally and almost flat-lined in strength after one week. The samples that were cured in 97% humidity did achieve the expected strength of almost 55MPa.

The static modulus tests gave an insight in the Young's modulus, resulting in E_{CEMI} = 33GPa and E_{CEMIII} = 28GPa. This 18% difference make sense when looking at the compressive test results, since these two properties are linked to each other. Due to the poor curing circumstances, especially the CEM III mixture is unable to hydrate properly, leading into a more porous concrete. The pores also lead to a more brittle material, meaning that the softening is less ductile compared to CEM I.

This test also gave compressive strengths of 24MPa and 17MPa, which is approximately 50% of the results of the compression tests. This difference was explained by the size effect of concrete, since these samples are almost double the height. Concrete contains many impurities, so increasing the size results in the chance of impurities being substantially higher. The concrete will then fail at its weakest point.

Lastly this experiment shows the high variance between the different LVDT's placed on the CEM III specimen. Not all sides of the concrete are exposed to the humidity equally, meaning some sides of the concrete become more porous. This causes local failure and even snap-back behaviour in one of the LVDT's.

The unreinforced three-point bending tests give tensile stresses of 3.40MPa and 2.81MPa, meaning a 21% lower strength for CEM III. This again can be explained by the higher porosity. Due to the lower strength and more brittle behaviour, the fracture energy is nearly 30% lower, meaning that it takes less energy for the BFS concrete to crack. The E-moduli were a surprising 38GPa and 31GPa, which are both higher than the compressive Young's moduli. This can be explained by the higher loading rate, influencing the static mechanical properties.

The reinforced four-point bending tests were supposed to give an indication on the bond strength between steel and concrete. The results are that the crack spacing for the reinforced CEM III beam are slightly lower, which would indicate a higher bond. Since the porosity of this beam is higher, the frictional resistance should be lower. This results can be explained by the human error in manufacturing the reinforcement cages. These cages are not consistent in both placement and quality of the steel, meaning that this results is not too reliable.

The last test was the water absorption test, resulting in consecutively 8.46% and 9.64% pores. When looking at the hydration speed and water loss of CEM III concrete, it is to be expected that the porosity is higher.

A summary of these results is given in figure 10.1. The properties of CEM I are all given as 100%, and the CEM III properties are given as a relative percentage to CEM I.

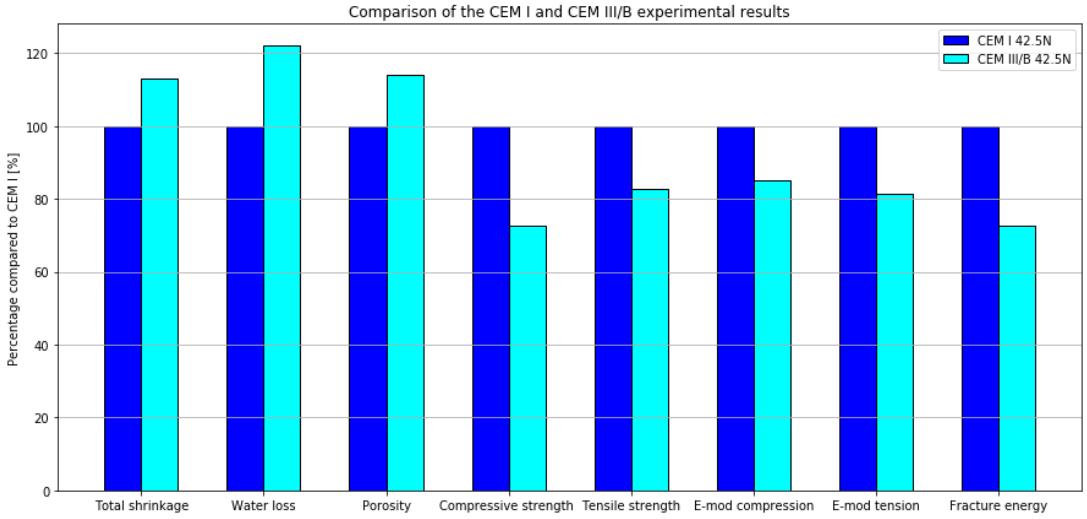

Figure 10.1: Relative results of CEM III/B compared to CEM I

To sum up all the results, the findings suggest that CEM III/B 42.5N concrete is much more susceptible to worse curing conditions than CEM I 42.5N concrete. Not only are all the mechanical properties about 15-30% worse, but the variance in their performance is higher as well. It can also be concluded that all the mechanical properties are connected. The larger amount of free water and porosity in the CEM III, results in more movement of the water, thus causing shrinkage. The higher porosity also results in less solid particles being available to provide strength and resistance, and explain the brittle behaviour as well.

The **second question** that has been answered is as follows:

What is the total effect on the life-cycle of a building when applying these different concrete mixtures, also considering sustainability?

To answer this question, the literature research and results from the experiments were used. New literature was also introduced in chapter 8, to determine the sustainability of producing and recycling the two different cements. Based on the mechanical properties, the effects on the construction and service life were described.

The total carbon emissions from producing CEM I, are 839 kg CO_2/t, compared to 342 kg CO_2/t for CEM III/B. Thus producing CEM I emits nearly 2.5 times as much carbon, which comes from the required energy for producing clinker.

The construction process becomes more difficult however, when applying CEM III concrete on the building site. When constructing a building with multiple in-situ floors, it would require four weeks of hardening to safely work on that floor. It would only take one week for CEM I concrete however. Due to the lower fracture energy, there is also a

higher likelihood of the blast furnace slag concrete experiencing early-stage cracks.

The largest effects can be found when considering the service life. Since all mechanical properties for CEM III/B have a lower value, the risk and maintenance increase, while the durability decreases. The higher porosity can allow for easier chloride ingress and moss growth. The lower Young's modulus would result in higher deformations, which means higher strengths or dimensions would need to be applied. Finally, due to the higher variance, it would be hard to make a reliable design. A construction is only as safe as its weakest link, meaning a higher variance could bring disastrous consequences.

Lastly, recycling CEM I would bring more gain than recycling CEM III, due to recycling clinker having a higher worth. For both concretes it is however still not feasible to recycle all aggregates and cement, since a lot of energy is required.

To conclude this research question, only the production process of CEM III/B is more sustainable. All other cycles of the building life are impacted negatively, resulting in unreliable and high maintenance infrastructure. This effect on durability will also impact the sustainability. This means that even though the production of CEM III/B is much more sustainable, application in practice will not be sustainable after all.

Overall conclusion

According to the research conducted in this thesis, it can thus be stated that the suboptimal curing conditions have a much higher impact on the mechanical properties of CEM III/B 42.5N, and thus also the life-cycle of a building. While previous literature suggests that CEM III concrete is both more sustainable and has better mechanical properties, this is certainly not the case for a 55% relative humidity environment. Based on the given results, CEM III/B should be treated carefully when implementing it in structures. In the given building site conditions, applying CEM I would be significantly more durable, cheaper, and especially safer.

11 Recommendations

Future research
When observing the results of this thesis, it becomes evident that further research into the effects of sub-optimal curing conditions is required. A list of recommendations is given below:

- When observing the specimen used for shrinkage, it can be seen that shrinkage for most of the specimen has not ceased after 75 days. Due to the time constraint, these specimen could not be tested longer, resulting in a 13% difference in total shrinkage. Since shrinkage is a long-term effect, a longer period should be considered to see the total effects. Based on the current results, half a year should give more reliable results, or until the shrinkage stops.
- To be able to isolate the effects of the relative humidity on the concrete properties, the water-to-cement ratio and types of aggregates were kept the same. In practice however, these parameters are surely not constant. To give a better understanding in the differences between CEM I 42.5N and CEM III/B 42.5N, the same experiments should be conducted where these effects are isolated. After that, mixtures should be made where all these parameters are randomized in a specific range. This way not only the effects of every single parameter can be found, but also the combinations.
- For some experiments like the three-point and four-point bending tests, only one specimen was tested for each material due to time/budget restrictions. To give a more reliable result and show the variance in the material, more specimen should be tested in the future.
- Not all relevant properties have been tested in these experiments. Some other properties that are significant for the durability and safety of a building are creep, thermal properties, fatigue and Poisson ratio. These properties should be tested in addition to the experiment conducted in this report.
- Due to the inexperience of making reinforcement cages, these were inconsistent for both concrete mixes. To accurately test the influence on the bond between the reinforcement and concrete in sub-optimal curing conditions, these cages should be made by a professional.

Recommendations for the building industry Based on the findings in this report, some recommendations can be made for the building industry, that will limit the damage of sub-optimal curing conditions.

- One possibility for achieving better mechanical properties with CEM III/B concrete, is putting the in-situ cast elements underwater for at least one week. When looking at the compressive strength gain in 97% humidity, even CEM III/B concrete nearly reaches the characteristic strength after seven days. Even assuming

a similar strength gain after one week as the cubes cured in 55% humidity, the minimum characteristic strength will easily be achieved.

- Since it is not always possible to put the concrete underwater, curing compounds are often used as a replacement. However, not all curing compounds are as effective as they are believed to be [103]. To have a reliable structure, the effectiveness of the used curing compound should be proven with tests.

- Since the relative humidity in the winter is quite high in The Netherlands, wind will have the highest impact on the internal relative humidity of the concrete. A solid solution for the more humid winter months would thus be to place wind breakers around the fresh concrete. This way the concrete is exposed to the high humidity, but is protected from the wind. In practice however, it might be hard to install wind breakers at certain locations.

- With weather forecasting becoming more and more accurate, a solution might also be to time the casting to the weather conditions. If a week of rain without too much wind is predicted, this might be a good time to cast. Even if it would not be practical to base the casting day on the weather conditions, it might still be useful to consider the forecast. If a sunny day is expected, some extra water can be sprayed on the concrete. If a lot of wind is expected, wind breakers or simply a sheet covering the concrete can be used.

References

[1] Polder, R., Nijland, T., Rooij, D., Larsen, C., & Pedersen, B. (2014). Innovation based on tradition: Blast furnace slag cement for durable concrete structures in Norway? TU Delft Repositories, 1. https://repository.tno.nl/islandora/object/uuid%3Ad0111fa5-a5ea-434e-83f0-91c9a3972f28

[2] Rezania, M., Panahandeh, M., Razavi, S. M. J., & Berto, F. (2019). Experimental study of the simultaneous effect of nano-silica and nano-carbon black on permeability and mechanical properties of the concrete. Theoretical and Applied Fracture Mechanics, 104, 102391. https://doi.org/10.1016/j.tafmec.2019.102391

[3] Yeih, W., Huang, R., Chang, J., & Yang, C. (1997). A pullout test for determining interface properties between rebar and concrete. Advanced Cement Based Materials, 5(2), 57–65. https://doi.org/10.1016/s1065-7355(96)00004-1

[4] K, N. S. (2017, December 7). Types of Shrinkages in Concrete and its Preventions. The Constructor. https://theconstructor.org/concrete/types-of-shrinkages-in-concrete-prevention/20384/

[5] Khayat, K. H. (1999). Workability, testing, and performance of Self-Consolidating Concrete. American Concrete Institute, Journal Of, 96(3). https://doi.org/10.14359/632

[6] Ha, J., Jung, Y., & Cho, Y. (2014). Thermal crack control in mass concrete structure using an automated curing system. Automation in Construction, 45, 16–24. https://doi.org/10.1016/j.autcon.2014.04.014

[7] Lee, J., & López, M. M. (2014). An experimental study on fracture energy of plain concrete. International Journal of Concrete Structures and Materials, 8(2), 129–139. https://doi.org/10.1007/s40069-014-0068-1

[8] What is the Right Water Cement Ratio — UltraTech. (n.d.). https://www.ultratechcement.com/for-homebuilders/home-building-explained-single/descriptive-articles/how-to-calculate-the-water-cement-ratio

[9] Concrete Construction. (1984). Control of air content. Concrete Construction, C840717.

[10] NEN-EN 206, Beton + NEN 8005, Nederlandse invulling van NEN-EN 206

[11] Happhoadmin. (2022, July 11). Bleeding of Concrete: Causes, Effect and Ways to Reduce it. Happho. https://happho.com/bleeding-concrete-causes-effect-ways-reduce/#:~:text=Bleeding%20occurs%20in%20concrete%20when,bleeding%20-channel%20will%20remain%20continues.

[12] Faci, K. B. P. P. (2022, August 4). Plastic shrinkage cracking in concrete - Causes and prevention. For Construction Pros. https://www.forconstructionpros.com/concrete/equipment-products/repair-rehabilitation-products/article/11487540/kb-engineering-llc-plastic-shrinkage-cracking-in-concrete-causes-and-prevention

[13] Yang, K., Zhong, M., Magee, B., Yang, C., Wang, C., Zhu, X., & Zhang, Z. (2017). Investigation of effects of Portland cement fineness and alkali content on concrete plastic shrinkage cracking. Construction and Building Materials, 144, 279–290. https://doi.org/10.1016/j.conbuildmat.2017.03.130

[14] En 197-1: Cement - part 1: Composition, specifications and conformity criteria for common cements.

[15] Vanoutrive, H., Van Den Heede, P., Alderete, N. M., Andrade, C., Bansal, T., Camões, A., Çizer, Ö., De Belie, N., Ducman, V., Etxeberria, M., Frederickx, L., Grengg, C., Ignjatović, I., Ling, T., Liu, Z., García-Lodeiro, I., Lothenbach, B., Medina, C., Montero, J. S., . . . Gruyaert, E. (2022). Report of RILEM TC 281-CCC: outcomes of a round robin on the resistance to accelerated carbonation of Portland, Portland-fly ash and blast-furnace blended cements. Materials and Structures, 55(3). https://doi.org/10.1617/s11527-022-01927-7

[16] Mishra, G. (2017, November 28). Types of Concrete Mix Ratio Design and their Strengths. The Constructor. https://theconstructor.org/concrete/types-of-concrete-mix-design/5984/#google_vignette

[17] A. Nayana and S. Kavitha, "Evaluation of c02 emissions for green concrete with high volume slag, recycled aggregate, recycled water to build eco environment," Int. J. Civ. Eng. Technol, vol. 8, pp. 703–708, 2017.

[18] Zemajtis, J. Z. (n.d.). Role of concrete curing. https://www.cement.org/learn/concrete-technology/concrete-construction/curing-in-construction

[19] Ježo, Ľubomir., Ifka, Tomas., Cvopa, B., Škundová, Janka., Kovár, V., & Palou, M. (2010). Effect of temperature upon the strength development rate and upon the hydration kinetics of cements. Ceram Silik, 54(3), 269-276.

[20] Neville, A., & Brooks, J. J. (1993). Concrete technology (Vol. 1993). http://library.um.ac.id/free-contents/index.php/buku/detail/concrete-technology-a-m-neville-j-j-brooks-657.html

[21] Aïtcin, P. (2016). Portland cement. In Elsevier eBooks (pp. 27–51). https://doi.org/10.1016/b978-0-08-100693-1.00003-5

[22] Kim, J., & Cs, L. (1998). Prediction of differential drying shrinkage in concrete. Cement and Concrete Research, 28(7), 985–994. https://doi.org/10.1016/s0008-8846(98)00077-5

[23] Demirboğa, R., & Farhan, K. Z. (2022). Palm oil fuel ash (POFA). In Elsevier eBooks (pp. 279–330). https://doi.org/10.1016/b978-0-12-824050-2.00006-1

[24] Mehta, P., & Monteiro, P. J. (2005). Concrete: microstructure, properties, and materials. http://ksaravind.yolasite.com/resources/P.K.Metha%20CONCRETE%20-%20microstructure%20properties%20and%20materials.pdf

[25] Abdelgader, H. S., Amran, M., Kurpińska, M., Mosaberpanah, M. A., Murali, G., & Fednok, R. (2022). Cement kiln dust. In Elsevier eBooks (pp. 451–479). https://doi.org/10.1016/b978-0-12-824050-2.00003-6

[26] Bolan, N., Srivastava, P., Rao, C. S., Satyanaraya, P., Anderson, G., Bolan, S., Nortjé, G. P., Kronenberg, R., Bardhan, S., Abbott, L. K., Zhao, H., Mehra, P., Satyanarayana, S., Khan, N., Wang, H., Rinklebe, J., Siddique, K. H. M., & Kirkham, M. (2023). Distribution, characteristics and management of calcareous soils. In Advances in agronomy (pp. 81–130). https://doi.org/10.1016/bs.agron.2023.06.002

[27] Rahman, F. U. (2017, 18 september). Manufacture of Cement- Materials and Manufacturing Process of Portland Cement. The Constructor. https://theconstructor.org/building/manufacture-of-cement/13709/

[28] Barrington, C. (n.d.). Pig iron - blast furnace route — International Iron Metallics Association. Copyright (C) 2024 by International Iron Metallics Association. https://www.metallics.org/pig-iron-bf.html

[29] Awoyera, P. O., Babalola, O. E., & Aluko, O. G. (2022). The use of slags in recycled aggregate concrete. In Elsevier eBooks (pp. 145–170). https://doi.org/10.1016/b978-0-12-824105-9.00009-3

[30] Faci, K. B. P. P. (2022b, August 4). Surface cracking caused by rapid moisture loss. For Construction Pros. https://www.forconstructionpros.com/concrete/article/21069289/kb-engineering-llc-surface-cracking-caused-by-rapid-moisture-loss

[31] Wyrzykowski, M., & Lura, P. (2016). Effect of relative humidity decrease due to self-desiccation on the hydration kinetics of cement. Cement and Concrete Research, 85, 75–81. https://doi.org/10.1016/j.cemconres.2016.04.003

[32] Zhang, H., Zhuang, J., Huang, S., Cheng, X., Hu, Q., Guo, Q., & Guo, J. (2015). Synthesis and performance of itaconic acid/acrylamide/sodium styrene sulfonate as a self-adapting retarder for oil well cement. RSC Advances, 5(68), 55428–55437. https://doi.org/10.1039/c5ra05167c

[33] Richardson, I. (1999). The nature of C-S-H in hardened cements. Cement and Concrete Research, 29(8), 1131–1147. https://doi.org/10.1016/s0008-8846(99)00168-4

[34] Portland Cement Association. (2001). Ettringite formation and the performance of concrete. https://www.cement.org/docs/default-source/fc_concrete_technology/is417-ettringite-formation-and-the-performance-of-concrete.pdf?sfvrsn=412%26sfvrsn=412

[35] G. Ye, Lectures CIE 5110 - Concrete Science and Technology. Technical University Delft, 2018.

[36] McCarthy, M. J., & Dyer, T. (2019). Pozzolanas and pozzolanic materials. In Elsevier eBooks (pp. 363–467). https://doi.org/10.1016/b978-0-08-100773-0.00009-5

[37] Cement. (2011). In Elsevier eBooks (pp. 46–423). https://doi.org/10.1533/9781845699567.46

[38] De Schutter, G., & Taerwe, L. (1995). General hydration model for portland cement and blast furnace slag cement. Cement and Concrete Research, 25(3), 593–604. https://doi.org/10.1016/0008-8846(95)00048-h

[39] Juilland, P., Gallucci, E., Flatt, R. J., & Scrivener, K. (2010). Dissolution theory applied to the induction period in alite hydration. Cement and Concrete Research (Print), 40(6), 831–844. https://doi.org/10.1016/j.cemconres.2010.01.012

[40] Stein, H., & Stevels, J. (1964). Influence of silica on the hydration of 3 CaO,SiO2. Journal of Applied Chemistry, 14(8), 338–346. https://doi.org/10.1002/jctb.5010140805

[41] Tadros, M. E., Skalny, J., & Kalyoncu, R. (1976). Early hydration of tricalcium silicate. Journal of the American Ceramic Society, 59(7–8), 344–347. https://doi.org/10.1111/j.1151-2916.1976.tb10980.x

[42] Fierens, P., & Verhaegen, J. (1976). Hydration of tricalcium silicate in paste — Kinetics of calcium ions dissolution in the aqueous phase. Cement and Concrete Research, 6(3), 337–342. https://doi.org/10.1016/0008-8846(76)90095-8

[43] Baxter, E. (2024, March 7). How cement mixers work. HowStuffWorks. https://science.howstuffworks.com/transport/engines-equipment/cement-mixer.htm

[44] Ortega, J. M., Pastor, J. L., Albaladejo, A., Sánchez, I., & Climent, M. (2014). Durability and compressive strength of blast furnace slag-based cement grout for special geotechnical applications. Materiales De Construcción, 64(313), e003. https://doi.org/10.3989/mc.2014.04912

[45] Globusog. (2016, November 30). Kinetics of cement hydration. https://www.globusogs.com/kinetics-of-cement-hydration/#prettyPhoto

[46] Xiao, J., Lv, Z., Duan, Z., & Zhang, C. (2023). Pore structure characteristics, modulation and its effect on concrete properties: A review. Construction & Building Materials, 397, 132430. https://doi.org/10.1016/j.conbuildmat.2023.132430

[47] Brouwers, H. J. (2004). The work of Powers and Brownyard revisited: Part 1. Cement and Concrete Research, 34(9), 1697–1716. https://doi.org/10.1016/j.cemconres.2004.05.031

[48] Maruyama, I. (2016). Multi-scale Review for Possible Mechanisms of Natural Frequency Change of Reinforced Concrete Structures under an Ordinary Drying Condition. Journal of Advanced Concrete Technology, 14(11), 691–705. https://doi.org/10.3151/jact.14.691

[49] Patel, R. A. (2016). Lattice Boltzmann method based framework for simulating physico-chemical processes in heterogeneous porous media and its application to cement paste. https://biblio.ugent.be/publication/8071415/file/8071428.pdf

[50] Artero, I. (2017, February 17). The water/cement ratio: a fragile relationship - Putzmeister. Putzmeister. https://bestsupportunderground.com/water-cement-ratio/?lang=en

[51] Ye, H. (2015). Creep Mechanisms of Calcium–Silicate–Hydrate: An Overview of recent advances and challenges. International Journal of Concrete Structures and Materials, 9(4), 453–462. https://doi.org/10.1007/s40069-015-0114-7

[52] Coatings, D., & Drinkwater, P. (2021, October 29). What is Capillary Action? D&D Coatings. https://www.ddcoatings.co.uk/3213/capillary-action

[53] Lu, T., Li, Z., & Van Breugel, K. (2020). Modelling of autogenous shrinkage of hardening cement paste. Construction & Building Materials, 264, 120708. https://doi.org/10.1016/j.conbuildmat.2020.120708

[54] Tang, S., Huang, D., & He, Z. (2021). A review of autogenous shrinkage models of concrete. Journal of Building Engineering, 44, 103412. https://doi.org/10.1016/j.jobe.2021.103412

[55] Daněk, P., Kucharczyková, B., Misák, P., & Kocáb, D. (2017). Experimental analysis on shrinkage and swelling in ordinary concrete. Advances in Materials Science and Engineering, 2017, 1–11. https://doi.org/10.1155/2017/3027301

[56] Löfgren, I. (2007). Calculation of crack width and crack spacing. ResearchGate. https://www.researchgate.net/publication/257944065_Calculation_of_crack_width_and_crack_spacing

[57] Material testing blog. (n.d.). https://certifiedmtp.com/blog?p=consistency-of-concrete-how-its-measured-why-its-important-and-relation-to-workability#:~:text=Consistency%20affects%20how%20well%20the,withstand%20the%20test%20of%20time.

[58] Factors affecting workability of concrete. (n.d.). Civil Engineering. https://civiltoday.com/civil-engineering-materials/concrete/94-factors-affecting-workability-of-concrete

[59] EPD International. (n.d.). https://www.environdec.com/home

[60] Li, Z., Delsaute, B., Lu, T., Kostiuchenko, A., Staquet, S., & Ye, G. (2021). A comparative study on the mechanical properties, autogenous shrinkage and cracking proneness of alkali-activated concrete and ordinary Portland cement concrete. Construction & Building Materials, 292, 123418. https://doi.org/10.1016/j.conbuildmat.2021.123418

[61] Basics of the Linear Variable Differential Transformer (LVDT) - RealPars. (n.d.). https://www.realpars.com/blog/lvdt

[62] Vonk, R. A. (1992). Softening of concrete loaded in compression. https://doi.org/10.6100/ir375705

[63] RILEM TC 148-SSC: STRAIN SOFTENING OF CONCRETE-TEST METHODS FOR COMPRESSIVE SOFTENING Test method for measurement of the strain-softening behaviour of concrete under uniaxial compression. (2000). https://www.semanticscholar.org/paper/RILEM-TC-148-SSC%3A-STRAIN-SOFTENING-OF-CONCRETE-TEST/b42d7fd8dc0293c387b50a674073902254a8b698

[64] Singh, K. (2023, April 17). Plasticizers for Concrete – Principle, Types & Advantages. Civil Engineering Portal - Biggest Civil Engineering Information Sharing Website. https://www.engineeringcivil.com/plasticizers-for-concrete-principle-types-advantages.html

[65] Feng, D., Wu, G., & Lu, Y. (2018). Finite element modelling approach for precast reinforced concrete beam-to-column connections under cyclic loading. Engineering Structures/Engineering Structures (Online), 174, 49–66. https://doi.org/10.1016/j.engstruct.2018.07.055

[66] Nirmaljoshi. (2018, November 15). Durability of concrete in terms of water permeability. Portal on Deterioration of RC Structures. https://18de154.wordpress.com/2018/11/15/durability-of-concrete-in-terms-of-water-permeability/

[67] What happens if concrete freezes during curing time? (2023, April 28). Converge. https://www.converge.io/blog/blog-what-happens-if-concrete-freezes

[68] Sandoval, G. F. B., Galobardes, I., Schwantes-Cezario, N., Campos, A., & Toralles, B. M. (2019). Correlation between permeability and porosity for pervious concrete (PC). https://www.redalyc.org/journal/496/49662418018/html/

[69] The Editors of Encyclopaedia Britannica. (1998, July 20). Young's modulus — Description, Example, & Facts. Encyclopedia Britannica. https://www.britannica.com/science/Youngs-modulus

[70] Kh, Hind & Özakça, Mustafa & Ekmekyapar, Talha. (2016). A Review on Nonlinear Finite Element Analysis of Reinforced Concrete Beams Retrofitted with Fiber Reinforced Polymers. 22. 2289-7895.

[71] Team, E. (n.d.). Table of concrete design properties (fcd, fctm, Ecm, fctd) - Eurocode 2. EurocodeApplied.com. https://eurocodeapplied.com/design/en1992/concrete-design-properties

[72] Krishnya, S., Yoda, Y., & Elakneswaran, Y. (2021). A two-stage model for the prediction of mechanical properties of cement paste. Cement & Concrete Composites, 115, 103853. https://doi.org/10.1016/j.cemconcomp.2020.103853

[73] Korolev, A. S., Kopp, A., Odnoburcev, D., Loskov, V., Shimanovsky, P., Koroleva, Y., & Vatin, N. I. (2021). Compressive and tensile elastic properties of concrete: Empirical factors in span Reinforced Structures Design. Materials, 14(24), 7578. https://doi.org/10.3390/ma14247578

[74] Farooq, M. A., Takeda, K., Sato, Y., & Niitani, K. (2017). Mechanical Properties of Concrete with Blast Furnace Slag Fine Aggregates Subjected to Freeze-Thaw Cycles. In Springer eBooks (pp. 65–72). https://doi.org/10.1007/978-3-319-59471-2_9

[75] Admin. (2023b, January 6). Poisson's ratio - longitudinal strain and lateral strain — BYJU'S. BYJUS. https://byjus.com/physics/poissons-ratio/

[76] Koratich, D. (n.d.). Drying shrinkage. https://www.engr.psu.edu/ce/courses/ce584/concrete/library/cracking/dryshrinkage/dryingshrinkage.html

[77] Ye, H., & Radlińska, A. (2016). A review and comparative study of existing shrinkage prediction models for Portland and Non-Portland cementitious materials. Advances in Materials Science and Engineering, 2016, 1–13. https://doi.org/10.1155/2016/2418219

[78] Murthy, A. R., Karihaloo, B., Iyer, N. R., & Prasad, B. R. (2013). Determination of size-independent specific fracture energy of concrete mixes by two methods. Cement and Concrete Research, 50, 19–25. https://doi.org/10.1016/j.cemconres.2013.03.015

[79] M. Elices, G.V. Guinea, J. Planas, Measurement of the fracture energy using three-point bend tests: part 3—influence of cutting the P– tail, Mater. Struct. 25 (1992) 137–163.

[80] G.V. Guinea, J. Planas, M. Elices, Measurement of the fracture energy using three-point bend tests: part 1—influence of experimental procedures, Mater. Struct. 25 (1992) 212–218.

[81] J. Planas, M. Elices, G.V. Guinea, Measurement of the fracture energy using three-point bend tests: part 2

[82] Kogbara, R. B., Iyengar, S. R., Grasley, Z. C., Masad, E. A., & Zollinger, D. G. (2013). A review of concrete properties at cryogenic temperatures: Towards direct LNG containment. Construction & Building Materials, 47, 760–770. https://doi.org/10.1016/j.conbuildmat.2013.04.025

[83] Faraj, R. H., Ahmed, H. U., Ali, H. F. H., & Sherwani, A. F. H. (2022). Fresh and mechanical properties of concrete made with recycled plastic aggregates. In Elsevier eBooks (pp. 167–185). https://doi.org/10.1016/b978-0-12-821730-6.00023-1

[84] Othman, Hesham. (2016). Performance of Ultra-High Performance Fibre Reinforced Concrete Plates under Impact Loads.

[85] Tanabe, T., Itoh, A., & Ueda, N. (2004). Snapback Failure Analysis for Large Scale Concrete Structures and its Application to Shear Capacity Study of Columns. Journal of Advanced Concrete Technology, 2(3), 275–288. https://doi.org/10.3151/jact.2.275

[86] Uday, N. P. (2017). Experimental determination of fracture energy by RILEM Method. The International Journal of Engineering and Science, 06(03), 106–115. https://doi.org/10.9790/1813-060301106115

[87] Talaat, A., Emad, A., Tarek, A., Masbouba, M., Essam, A., & Kohail, M. (2021). Factors affecting the results of concrete compression testing: A review. Ain Shams Engineering Journal/Ain Shams Engineering Journal, 12(1), 205–221. https://doi.org/10.1016/j.asej.2020.07.015

[88] Collins, M. (n.d.). Characteristic strength. https://www.concrete.org.uk/fingertips-document.asp?id=1055

[89] Hansen, U., Zioupos, P., Simpson, R., Currey, J. D., & Hynd, D. (2008). The effect of strain rate on the mechanical properties of human cortical bone. Journal of Biomechanical Engineering, 130(1). https://doi.org/10.1115/1.2838032

[90] Bian, H., Wang, F., Chen, W., & Wang, H. (2023). Study on dynamic and static elastic moduli of shale oil by different loading methods. Unconventional Resources, 3, 183–191. https://doi.org/10.1016/j.uncres.2023.03.002

[91] Fan, L., Wong, L., & Ma, G. (2013). Experimental investigation and modeling of viscoelastic behavior of concrete. Construction & Building Materials, 48, 814–821. https://doi.org/10.1016/j.conbuildmat.2013.07.010

[92] Prakasan, S., Palaniappan, S., & Gettu, R. (2019). Study of energy use and CO2 emissions in the manufacturing of clinker and cement. Journal of Institution of Engineers Series A, 101(1), 221–232. https://doi.org/10.1007/s40030-019-00409-4

[93] https://www.formingamerica.com/how-long-should-concrete-cure-before-putting-weight-on-it/#:~:text=Here%20are%20the%20average%20times,cured%20and%20at%20peak%20durability

[94] Zajac M., Evaluation, energy demand and environmental impact of cement production process, research paper of Heidelberg cement group, 2009.

[95] Building Materials and the climate: Constructing a new future. (n.d.). UNEP - UN Environment Programme. https://www.unep.org/resources/report/building-materials-and-climate-constructing-new-future

[96] Li, Z., Delsaute, B., Lu, T., Kostiuchenko, A., Staquet, S., & Ye, G. (2021b). A comparative study on the mechanical properties, autogenous shrinkage and cracking proneness of alkali-activated concrete and ordinary Portland cement concrete. Construction & Building Materials, 292, 123418. https://doi.org/10.1016/j.conbuildmat.2021.123418

[97] A field-scale analysis of the dependence of wind erosion threshold velocity on air humidity - Scientific Figure on ResearchGate. Available from: https://www.researchgate.net/figure/Relative-humidity-RH-as-a-function-of-wind-speed-v-for-the-four-stations-all-data_fig3_241060910

[98] TU Delft OpenCourseWare. (2020, March 23). 3.1.2 Life-Cycle of a Building - TU Delft OCW. TU Delft OCW. https://ocw.tudelft.nl/course-readings/3-1-2-life-cycle-of-a-building/

[99] Relative humidity, current observations Netherlands. (n.d.). Meteologix.com. https://meteologix.com/nl/observations/humidity.html

[100] Verkennend onderzoek naar betonaantasting in combinatie met mosaangroei - CROW. (n.d.). https://www.crow.nl/publicaties/verkennend-onderzoek-naar-betonaantasting-in-combi

[101] Concrete recycling. (n.d.). TU Delft. https://www.tudelft.nl/citg/over-faculteit/afdelingen/engineering-structures/sections-labs/resources-recycling/research-innovation/recycling-technologies/concrete-recycling

[102] Diving into Steelmaking Routes: From Blast Furnace to Electric Arc Furnace. (2024, April 9). https://blog.cabaro-group.com/diving-into-steelmaking-routes-from-blast-furnace-to-electric-arc-furnace/

[103] Chyliński, F., Michalik, A., & Kozicki, M. (2022). Effectiveness of curing compounds for concrete. Materials, 15(7), 2699. https://doi.org/10.3390/ma15072699

[104] Annual wind speed Averages for the Netherlands - Current results. (n.d.). https://www.currentresults.com/Weather/Netherlands/wind-speed-annual.php

[105] Mier, van, J. G. M. (1984). Strain-softening of concrete under multiaxial loading conditions. [Phd Thesis 1 (Research TU/e / Graduation TU/e), Built Environment]. Technische Hogeschool Eindhoven. https://doi.org/10.6100/IR145193

A Test results tables

A.1 Shrinkage

	Specimen 1		Specimen 2		Specimen 3	
Days	Length [mm]	Weight [g]	Length [mm]	Weight [g]	Length [mm]	Weight [g]
1	284.1750	3787.6	284.1830	3695.0	284.1590	3775.5
2	284.1660	3744.8	284.1770	3661.1	284.1510	3739.4
3	284.1625	3729.9	284.1720	3635.2	284.1455	3717.2
6	284.1440	3719.6	284.1530	3623.0	284.1280	3703.2
7	284.1365	3717.3	284.1475	3620.7	284.1210	3700.0
9	284.1325	3713.5	284.1415	3616.7	284.1160	3695.9
14	284.1230	3706.9	284.1300	3610.4	284.1040	3689.8
15	284.1235	3705.9	284.1300	3609.4	284.1040	3688.8
21	284.1170	3700.9	284.1245	3604.6	284.1000	3684.6
27	284.1135	3697.2	284.1210	3600.8	284.0950	3681.2
30	284.1120	3696.5	284.1190	3600.0	284.0925	3680.6
36	284.1085	3695.2	284.1155	3598.6	284.0880	3679.4
43	284.1060	3694.0	284.1125	3597.4	284.0855	3678.2
49	284.1040	3693.7	284.1100	3596.9	284.0820	3677.8
68	284.1020	3693.1	284.1075	3596.4	284.0800	3677.2
75	284.1020	3693.0	284.1070	3596.2	284.0790	3677.0

Table A.1: Total shrinkage CEM I

	Specimen 1		Specimen 2		Specimen 3	
Days	Length [mm]	Weight [g]	Length [mm]	Weight [g]	Length [mm]	Weight [g]
1	284.2070	3919.5	284.1155	3960.1	284.1410	3988.4
2	284.2080	3918.8	284.1145	3959.6	284.1410	3987.7
3	284.2040	3918.4	284.1105	3959.2	284.1380	3987.3
6	284.2015	3917.8	284.1085	3958.5	284.13345	3986.8
7	284.1995	3917.6	284.1065	3958.4	284.1335	3986.6
9	284.1985	3917.4	284.1055	3958.4	284.1320	3986.6
14	284.1960	3916.9	284.1025	3957.9	284.1290	3986.1
15	284.1945	3916.8	284.1020	3957.7	284.1280	3986.0
21	284.1935	3916.3	284.1000	3957.2	284.1265	3985.6
27	284.1930	3915.9	284.0990	3956.7	284.1255	3985.2
30	284.1920	3915.6	284.0990	3956.5	284.1250	3985.0
36	284.1910	3915.3	284.0975	3956.2	284.1245	3984.7
43	284.1900	3914.9	284.0960	3955.9	284.1235	3984.3
49	284.1890	3914.5	284.0950	3955.5	284.1225	3984.0
68	284.1875	3913.8	284.0935	3955.0	284.1210	3983.6
75	284.1870	3913.6	284.0930	3954.8	284.1210	3983.5

Table A.2: Autogenous shrinkage CEM I

	Specimen 1		Specimen 2		Specimen 3	
Days	Length [mm]	Weight [g]	Length [mm]	Weight [g]	Length [mm]	Weight [g]
1	284.1885	3688.9	284.0040	3690.8	284.1225	3708.1
4	284.1840	3608.5	283.9915	3612.9	284.1170	3596.7
5	284.1750	3604.8	283.9830	3609.8	284.1060	3594.2
7	284.1495	3600.0	283.9675	3603.2	284.0880	3590.6
12	284.1350	3597.1	283.9580	3598.6	294.0740	3586.7
13	284.1325	3596.2	283.9550	3597.4	284.0705	3586.2
19	284.1185	3591.1	283.9405	3592.3	284.0580	3583.4
25	284.1135	3587.5	283.9375	3588.9	284.0525	3581.0
28	284.1100	3586.5	283.9345	3588.1	284.0485	3580.5
34	284.1065	3584.8	283.9305	3586.5	284.0460	3579.6
41	284.1030	3583.3	283.9275	3584.8	284.0445	3578.0
47	284.1010	3581.9	283.9250	3583.7	284.0420	3576.9
66	284.0975	3578.9	283.9220	3580.9	284.0390	3574.1
73	284.0965	3577.9	283.9215	3580.0	284.0380	3573.1

Table A.3: Total shrinkage CEM III

	Specimen 1		Specimen 2		Specimen 3	
Days	Length [mm]	Weight [g]	Length [mm]	Weight [g]	Length [mm]	Weight [g]
1	284.2870	3893.9	284.0325	3908.4	284.2560	3913.3
4	284.2850	3892.7	284.0300	3907.9	284.2535	3912.7
5	284.2785	3892.6	284.0240	3907.9	284.2490	3912.6
7	284.2735	3892.6	284.0195	3908.0	284.2435	3912.6
12	284.2665	3892.5	284.0145	3907.7	284.2380	3912.5
13	284.2650	3892.5	284.0135	3907.7	284.2365	3912.5
19	284.2600	3892.2	284.0080	3907.4	284.2305	3912.2
25	284.2575	3892.0	284.0050	3907.0	284.2270	3911.9
28	284.2550	3891.9	284.0025	3907.0	284.2250	3911.8
34	284.2535	3891.8	284.0015	3906.8	284.2225	3911.6
41	284.2525	3891.6	284.0000	3906.5	284.2210	3911.3
47	284.2515	3891.3	283.9990	3906.2	284.2205	3911.1
66	284.2500	3891.0	283.9970	3905.8	284.2180	3910.8
73	284.2500	3891.0	283.9965	3905.8	284.2175	3910.7

Table A.4: Autogenous shrinkage CEM III

A.2 Compression

Days	Concrete using CEM I 42.5N Compressive strength [MPa]	Concrete using CEM III/B 42.5N Compressive strength [MPa]
1	11.53	3.23
	11.78	3.40
	11.63	3.34
Mean±std	**11.65±0.10**	**3.32±0.07**
3	31.27	18.65
	29.22	19.23
	30.31	18.88
Mean±std	**30.27±0.84**	**18.92±0.24**
7	42.31	31.09
	41.61	32.81
	40.84	32.21
Mean±std	**41.59±0.60**	**32.04±0.71**
14	43.50	38.30
	45.00	36.10
	46.43	34.86
Mean±std	**44.98±1.20**	**36.42±1.42**
28	51.96	33.27
	46.84	40.23
	52.91	35.84
Mean±std	**50.57±2.67**	**36.45±2.87**
56	54.00	40.77
	49.80	42.05
	55.49	36.74
Mean±std	**53.10±2.41**	**39.85±2.26**

Table A.5: Cube compression test results 55% humidity

Days	Concrete using CEM I 42.5N Compressive strength [MPa]	Concrete using CEM III/B 42.5N Compressive strength [MPa]
1	11.58	3.32
	11.90	3.50
Mean±std	**11.74±0.16**	**3.41±0.09**
3	34.93	22.94
	35.39	21.95
Mean±std	**35.16±0.23**	**22.45±0.495**
7	43.94	39.01
	45.71	40.29
Mean±std	**44.84±0.87**	**39.65±0.64**
14	47.65	47.91
	49.63	45.16
Mean±std	**48.64±0.99**	**46.54±1.375**
28	51.98	52.75
	55.42	55.45
Mean±std	**53.70±1.72**	**54.10±1.35**

Table A.6: Cube compression test results 97% humidity

A.3 Porosity

For CEM I 42.5N:

$$W_{total} = 3723.7g \tag{A.1}$$

$$W_{dry} = 3570.2g \tag{A.2}$$

$$W_{wet} = W_{total} - W_{dry} = 153.7g \tag{A.3}$$

$$V_w = \frac{W_{wet}}{\rho_{water}} = \frac{0.1537}{1000} = 1.537 * 10^{-4} m^3 \tag{A.4}$$

$$V_t = l * b * h = 0.08 * 0.08 * 0.284 = 1.82 * 10^{-3} m^3 \tag{A.5}$$

$$\phi = \frac{V_w}{V_t} * 100\% = 8.46\% \tag{A.6}$$

For CEM III/B 42.5N:

$$W_{total} = 3719.3g \tag{A.7}$$

$$W_{dry} = 3544.2g \tag{A.8}$$

$$W_{wet} = W_{total} - W_{dry} = 175.1g \tag{A.9}$$

$$V_w = \frac{W_{wet}}{\rho_{water}} = \frac{0.1751}{1000} = 1.751 * 10^{-4} m^3 \tag{A.10}$$

$$V_t = l * b * h = 0.08 * 0.08 * 0.284 = 1.82 * 10^{-3} m^3 \tag{A.11}$$

$$\phi = \frac{V_w}{V_t} * 100\% = 9.64\% \tag{A.12}$$